Do Muscles Constrain Skull Shape Evolution in Strepsirrhines?

ANNE-CLAIRE FABRE [1]* JONATHAN M. G. PERRY [2] ADAM HARTSTONE-ROSE [3] AURÉLIEN LOWIE,[1] ANDY BOENS,[1] AND MAÏTENA DUMONT[1,4]

[1]UMR 7179, Département Adaptations du Vivant, Museum National d'Histoire Naturelle, Centre National de la Recherche Scientifique, 75005 Paris, France
[2]Center for Functional Anatomy and Evolution, The Johns Hopkins University School of Medicine, Baltimore, Maryland
[3]College of Science, North Carolina State University, Raleigh, North Carolina
[4]Uppsala Universitet, Uppsala, Sweden

ABSTRACT

Despite great interest and decades of research, the musculoskeletal relationships of the masticatory system in primates are still not fully understood. However, without a clear understanding of the interplay between muscles and bones it remains difficult to understand the functional significance of morphological traits of the skeleton. Here, we aim to study the impacts of the masticatory muscles on the shape of the cranium and the mandible as well as their co-variation in strepsirrhine primates. To do so, we use 3D geometric morphometric approaches to assess the shape of each bone of the skull of 20 species for which muscle data are available in the literature. Impacts of the masticatory muscles on the skull shape were assessed using non-phylogenetic regressions and phylogenetic regressions whereas co-variations were assessed using two-blocks partial least square (2B-PLS) and phylogenetic 2B-PLS. Our results show that there is a phylogenetic signal for skull shape and masticatory muscles. They also show that there is a significant impact of the masticatory muscles on cranial shape but not as much as on the mandible. The co-variations are also stronger between the masticatory muscles and cranial shape even when taking into account phylogeny. Interestingly, the results of co-variation between the masticatory muscles and mandibular shape show a more complex pattern in two different directions to get strong muscles associated with mandibular shape: a folivore way (with the bamboo lemurs and sifakas) and a hard-object eater one (with the aye-aye). Anat Rec, 301:291–310, 2018. © 2018 Wiley Periodicals, Inc.

Key words: muscle; adaptation; vertebrates; masticatory system; primates

Additional Supporting Information may be found in the online version of this article.

Grant sponsor: Marie-Skłodowska Curie fellowship; Grant number: EU project 655694 – GETAGRIP.

*Correspondence to: Anne-Claire Fabre Muséum National d'Histoire Naturelle, 55 rue Buffon, 75005 Paris, France. e-mail: fabreac@gmail.com and anne-claire.fabre@mnhn.fr

Marie-Skłodowska Curie fellowship (EU project 655694 – GETAGRIP) for funding.

Received 10 February 2017; Revised 27 July 2017; Accepted 24 August 2017.

DOI 10.1002/ar.23712
Published online in Wiley Online Library (wileyonlinelibrary.com).

The interrelationships of bones and muscles of the vertebrate skeleton (i.e. musculoskeletal configuration) are both constrained and shaped by force and motion (Currey, 2002). The relationships between musculoskeletal anatomy and ecology have also been explored, yet are often more diffuse (Bock and von Wahlert, 1965; Polly, 2008). On one hand, a given musculoskeletal configuration must be compatible with the size and habits of the organism, and as such is likely adapted to its habitat and general environment. On the other hand, musculoskeletal configuration is often flexible and must be able to cope with diverse environmental demands. Even if an organism's musculoskeletal configuration is somewhat plastic and can be modified during its lifetime (Renaud et al., 2010) it is predominantly heritable (Cock, 1966; Grüneberg, 1967; Thorpe, 1981; Polly, 2008). Evolutionary change over time thus requires generations of selective genetic and/or epigenetic reorganization. The temporal lag of phylogenetic adaptation and the many-to-many relationships between form, function, and habitat (Polly, 2008) imply that the relationship between a given musculoskeletal configuration and the ecology of an organism is often rather coarse. A major problem that remains to be analyzed then, is how the interplay between bones and muscles in a phylogenetic context can be better understood and can enlighten the evolution of organisms in their environmental context.

Unfortunately, bones and muscles are often studied separately (Viguier, 2002, 2004; Perry et al., 2011; Singh et al., 2012; Baab et al., 2014; Noback and Harvati, 2015; Terhune et al., 2015; Dumont et al., 2016) and rarely jointly (Cornette et al., 2013, 2015; Fabre et al., 2014a). This is particularly problematic for those of us interested in reconstructing the muscular anatomy (and the behaviors that they allow) in extinct taxa (e.g., Perry et al., 2015); without a more comprehensive understanding of the relationship between muscles and bones in living species, we cannot hope to understand the muscles and muscular abilities of extinct species for which all our knowledge comes from fossils. Here, we want to investigate the interplay between the skull shape (cranium and mandible) and the mechanical and architectural constraints imposed by the masticatory muscles. The mammalian skull is a complex and highly integrated system (Wake and Roth, 1989; Hanken and Hall, 1993) which is composed of two or three mobile elements that are mainly interacting during feeding and other oral behaviors. In order to study the relationships between the skull and the masticatory muscles, we will focus on the strepsirrhine primates. This suborder is a good model group due to the fact that it includes a large number of species with a great diversity of behaviors, ecologies, and morphologies. Furthermore, its phylogeny is well-documented allowing us to take the evolutionary relationships between species into account in our analyses.

To investigate the evolutionary co-variation between the skull shape and the masticatory muscles we will explore the co-variation between the shape of the cranium and the mandible and the mechanical (using physiological cross-sectional area [PCSA]) and architectural (volume) constraints imposed by the masticatory muscles. This approach will help us to understand how the cranial and mandibular shape co-vary with the mechanical and architectural demands of masticatory muscles. We predict that the mandibular shape, which mainly has one function, i.e., biting, will have greater co-variation with the PCSA of the masticatory muscles because it reflects more the mechanical constraints imposed during biting (bone remodeling to reinforce the mandible). The cranium, on the other hand, is implicated in many more functions, and as such is expected to co-vary more with volume of the masticatory muscles, because it reflects the architectural constraint that are imposed by the space needed to accommodate muscles.

MATERIAL AND METHODS

Material

The dataset is composed of the skull (cranium and mandible) of 59 individuals belonging to two species of

TABLE 1. Details of specimens used in analyses with family, species names, common names and number of individuals (N)

Family	Species	Common name	N
Cheirogaleidae	*Cheirogaleus medius*	Fat-tailed dwarf lemur	4
	Microcebus murinus	Gray mouse lemur	3
Daubentoniidae	*D. madagascariens*	Aye-aye	4
Galagidae	*O. crassicaudatus*	Greater galago	6
	Otolemur garnettii	Small-eared galago	1
	G. demidoff	Prince Demidoff's bushbaby	1
	Galago senegalensis	Senegal galago	1
Indriidae	*Propithecus coquereli*	Coquerel's sifaka	4
	Propithecus diadema	Diademed sifaka	2
Lemuridae	*Eulemur collaris*	Red-collared lemur	2
	Eulemur coronatus	Crowned lemur	5
	Eulemur flavifrons	Blue-eyed black lemur	3
	Eulemur mongoz	Mangoose lemur	5
	Eulemur rubriventer	Red-bellied lemur	2
	Hapalemur griseus	Bamboo lemur	3
	Lemur catta	Ring-tailed lemur	3
	Varecia rubra	Red ruffed-lemur	2
Lorisidae	*Nycticebus coucang*	Slow loris	5
	Nycticebus pygmaeus	Pygmy slow loris	2
	Perodicticus potto	Potto	1

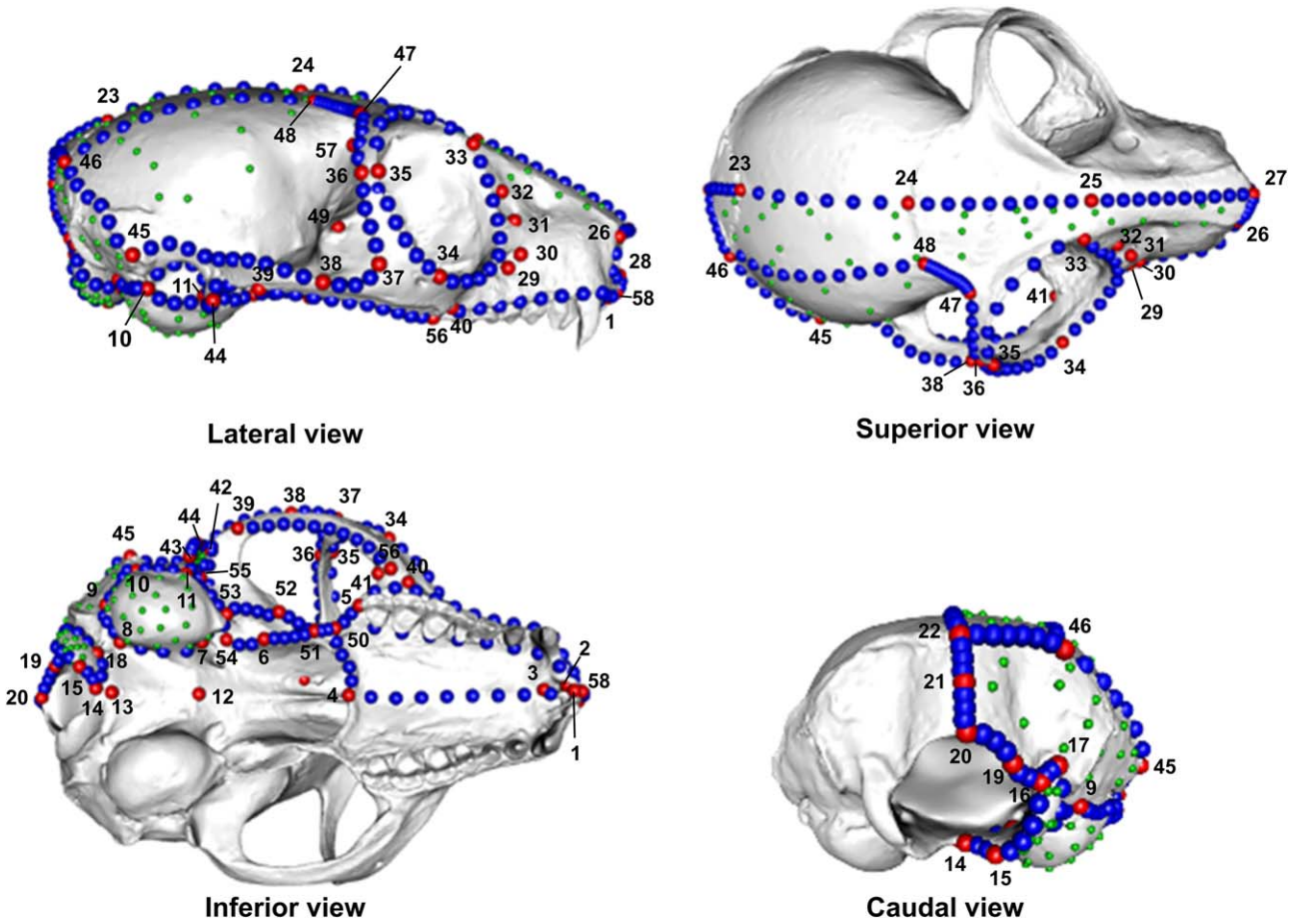

Fig. 1. Landmarks used in our analyses to quantify cranial shape variation. Red points represent homologous landmarks; blue points represent sliding-semilandmarks of curves, and light green points sliding-semilandmarks on surfaces.

Cheirogaleidae, one species of Daubentoniidae, four species of Galagidae, two species of Indriidae, eight species of Lemuridae, and three species of Lorisidae (Table 1, Supporting Information Table S1). For each species, the number of specimens ranged from one to six (Table 1). Where possible we selected specimens of wild caught origin, and equal numbers of males and females were included. Specimens were obtained from the Collections d'Anatomie Comparée, Muséum National d'Histoire Naturelle (MNHN), Paris, France; from the Royal Museum for Central Africa, Tervuren, Belgium as well as from the online data-archive Morphosource, and the Smithsonian National Museum of Natural History (http://humanorigins.si.edu/evidence/3d-collection/primate) Washington, District of Columbia. See supplementary Table S1 for a complete list of the specimens used in the analyses. All the bones from the MNHN and Tervuren were digitized using a Breuckmann 3D surface scanner at the MNHN, Paris. This surface scanner allows the acquisition of the 3D surface of the bone at high resolution using white light fringes (StereoSCAN^{3D} model with a camera resolution of five megapixels). Digital scans of bones from online repositories were downloaded with permission.

METHODS

Quantification of Shape Using 3D Geometric Morphometrics

The shape of the cranium and mandible are complex and cannot be adequately represented using a traditional landmark-based approach (Fabre et al., 2013a, 2013b, 2014b, 2015a, 2015b). Consequently, a 3D sliding-semilandmark procedure (Bookstein, 1997; Gunz et al., 2005) was used to quantify their morphology, and especially the areas of attachment of masticatory muscles. Through this procedure, sliding-semilandmarks on surfaces and curves are transformed into geometrically (i.e. spatially) homologous landmarks that can be used to compare shapes (Parr et al., 2012). Semilandmarks are allowed to slide along the curves and surfaces that are predefined while minimizing bending energy. Anatomical landmarks and sliding-semilandmarks of curves were obtained on 3D surface scans of each bone using the software package Idav Landmark (Wiley et al., 2005), while the library "Morpho" (Schlager, 2013) in R (Hornik, 2015) was used to perform the sliding-semilandmark procedure. To do so, we first created a template for each bone following the method of Cornette

TABLE 2. Definition of the landmarks of the cranium used in the geometric morphometric analyses

Landmark	Definition
1	Most antero-inferior point in the middle of the incisors row in the premaxilla, middle
2	Most anterior point of the incisive foramen
3	Most posterior point of the incisive foramen
4	Most posterior point in the middle of the palatine, middle
5	Most latero-posterior point of the maxilla
6	Tip of the medial pterygoid plate
7	Most cranial point of the tympanic bulla on the basisphenoid
8	Point at the maximum of curvature at the medio-posterior part of the tympanic bulla
9	Most posterior point of the tympanic bulla
10	Most posterior point of the external auditory meatus
11	Most anterior point of the external auditory meatus
12	Point of contact at the basioccipital-basisphenoid suture, middle
13	Most anterior point of the pharyngeal tubercle, middle
14	Most inferior point on the foramen magnum, middle
15	Point of maximum of curvature on the medio-inferior side of the occipital condyle
16	Most superior point of the jonction between the occypital condyle and the foramen magnum
17	Most latero-superior point of the occipital condyle
18	Point of maximum of curvature in latero-inferior part of the occipital condyle
19	Point of maximum of curvature between the most superior point of the foramen magnum and the occipital condyle
20	Most superior point on the foramen magnum, middle
21	Point of maximum of curvature between the point 22 and 20, middle
22	Most prominent point of the occipital bone, middle
23	Point of contact at the parietal-occipital suture, middle
24	Point of contact at the frontal-parietal suture, middle
25	Point of contact at the nasal-frontal sutures, middle
26	Most anterior point of contact at the nasal-premaxilla suture
27	Point of contact at the nasal sutures, middle
28	Most antero-superior point in the middle of the incisors row in the premaxilla, middle
29	Most inferior point of the infraorbital foramen
30	Most superior point of the infraorbital foramen
31	Most inferior point of the lacrimal foramen
32	Most superior point of the lacrimal foramen
33	Most medial point of the orbit
34	Most ventral point of the orbit
35	Most anterior point of contact on the sutures of the zygomatic-frontal bones on the postorbital bar
36	Most posterior point of contact on the sutures of the zygomatic-frontal bones on the postorbital bar
37	Point of maximum of curvature between the postorbital bar and zygomatic arch
38	Most superior point of contact at the jugual-squamosal suture
39	Most inferior point at the jugal-squamosal suture
40	Most anterior point of insertion of the jugual on the maxilla
41	Most posterior point of insertion of the jugual on the maxilla
42	Most antero-lateral point of the glenoid cavity
43	Most postero-medial point of the glenoid cavity
44	Most postero-lateral point of the glenoid cavity
45	Most lateral point of the nuchal crest
46	Most prominent point on the nuchal crest
47	Most superior point of insertion of the postorbital bar on the braincase
48	Point of contact on the sutures of the parietal and the frontal, at the beginning of the temporal line
49	Point at the top of the rotundum foramen
50	Most postero-medial point at the palatine-maxilla suture
51	Point at the palatine-pterygoid suture
52	Tip of the lateral pterygoid plate
53	Point of insertion of the lateral pterygoid plate on the pterygoid fossa
54	Point of insertion of the medial pterygoid plate on the pterygoid fossa
55	Most antero-medial point of the glenoid cavity
56	Most lateral point of insertion of the jugal on the maxilla
57	Most inferior point of insertion of the postorbital bar on the braincase
58	Most antero-superior point in the middle of the incisors row in the premaxilla, middle

et al. (2013) with 58 anatomical landmarks, 238 sliding-semilandmarks on curves and 105 sliding-semilandmarks on surfaces for the cranium; 20 anatomical landmarks, 120 sliding-semilandmarks on curves and 34 sliding-semilandmarks on the surface for the mandible. In this procedure each specimen is first defined by homologous landmark coordinates, which consisted of 58 landmarks for the cranium (Fig. 1 and Table 2) and 20 landmarks for the mandible (Fig. 2 and Table 3). Two-hundred-thirty-eight sliding-semilandmarks on curves were defined for the cranium (see Fig. 1) and 120 for the mandible (see Fig. 2). All these curves are constrained

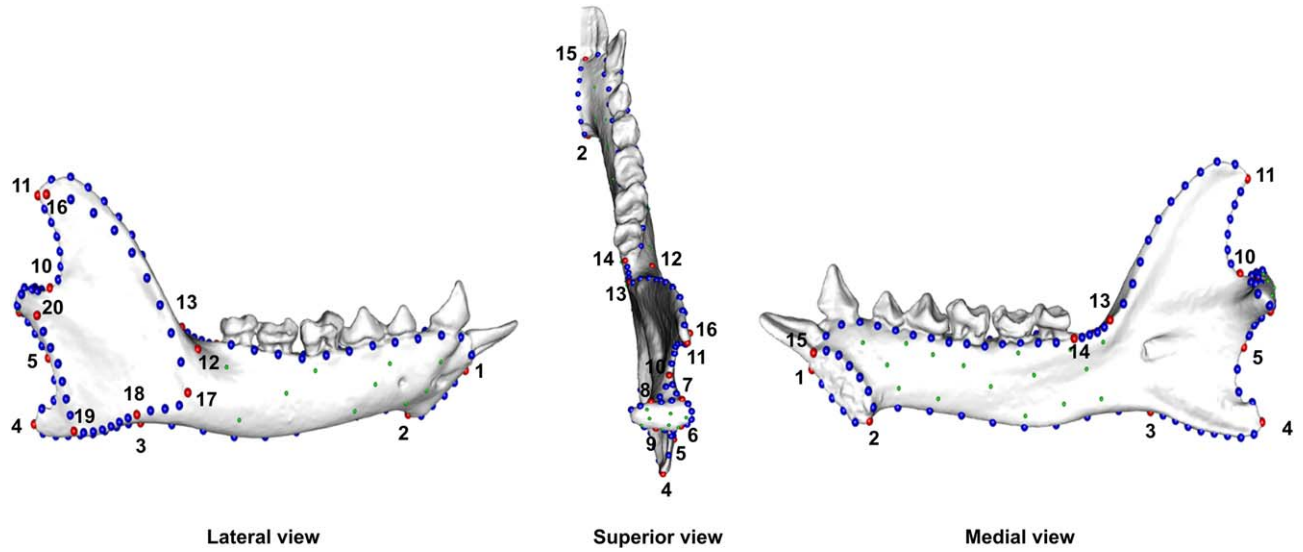

Fig. 2. Landmarks used in our analyses to quantify mandibular shape variation. Red points represent homologous landmarks; blue points represent sliding-semilandmarks of curves, and light green points sliding-semilandmarks on surfaces.

by homologous landmarks (see Gunz et al., 2005). Based on the homologous landmarks and curves taken on the specimen, all the sliding-semilandmarks (curve and surface sliding-semilandmarks) of the template are projected onto the new specimen using a thin plate spline deformation (Gunz and Mitteroecker, 2013). Finally, spline relaxation must be performed. Both sliding and relaxation are repeated iteratively until the bending energy is minimized. All these steps were performed using the library "Morpho" (Schlager, 2013) that follows the algorithm of Gunz et al. (2005), which is implemented in R (Hornik, 2015). At the end, four thin-plate spline relaxations were performed, the first relaxation was performed against the template, and the three others against a Procrustes consensus calculated using the data from the previous iteration. After this operation has been performed, the landmarks of all specimens can be compared using traditional geometric morphometric methods.

Once all landmark data were obtained, a generalized Procrustes superimposition (Rohlf and Slice, 1990) was performed using the library "Geomorph" (Adams and Otarola-Castillo, 2013) in R (Hornik, 2015). A mean shape was calculated for each species using the Procrustes coordinates and used in all further analyses. A Principal Component Analysis (PCA) was performed on the shape data of each bone of the skull. Finally, the first three principal components (accounting for more than 85% of variance for the mandible and 61% of the variance for the cranium) are used in all regression analyses.

TABLE 3. Definition of the landmarks of the mandible used in the geometric morphometric analyses

Landmark	Definition
1	Most antero-superior point of the mandibular symphysis, middle
2	Most postero-inferior point of the mandibular symphysis, middle
3	Most superior point on the inferior border of the ramus
4	Point at the tip of the angular process
5	Most anterior point on the curve of the posterior edge of the mandible
6	Most postero-lateral point of the condyle
7	Most antero-lateral point of the condyle
8	Most antero-medial point of the condyle
9	Most postero-medial point of the condyle
10	Most concave point of the incisura mandibulare
11	Point at the tip of the coronoid process
12	Point of insertion of the coronoid process on the ramus on the lateral side
13	Point of insertion of the coronoid process on the ramus on the medial side
14	Most posterior point on the molar row
15	Most postero-superior point of the mandibular symphysis, middle
16	Most lateral point of the coronoid process
17	Anterior edge of the masseteric ridge
18	Infero-posterior most point of the superficial masseter
19	Most onferior point of the angular process
20	Posterior edge of the masseteric ridge

Quantification of Muscles of the Cranium

PCSA and muscle masses were obtained from the literature (Perry et al., 2011, 2014) for the following muscles: deep masseter (DM), deep temporalis (DT), medial pterygoid (MP), superficial masseter (SM), superficial temporalis (ST), zygomatico-mandibularis (ZM), temporalis pars suprazygomatica (ZT).

Quantification of the Procrustes Variance (Disparity) of the Cranial and Mandibular Shape

In order to assess the variance of the cranial and mandibular shape, the disparity was measured using the Procrustes variance. To do so, we used the function

'morphol.disparity' of the 'geomorph' library (Zelditch et al., 2012; Adams and Otarola Castillo, 2013) in R (Hornick, 2015).

Phylogeny

The phylogenetic tree of strepsirrhines used in our analyses is a time-calibrated phylogeny obtained from the recent publication by Herrera and Dávalos (2016). This tree was used in all comparative analyses.

Phylogenetic Signal

To estimate the phylogenetic signal in the cranial and mandibular shape as well as in the muscle dataset we used a randomization test following the method of Blomberg et al. (2003) and the extended methods of Adams (2014). A multivariate K-statistic (Adams, 2014) was calculated based on the mean of the Procrustes coordinate of each species for the shape of each bone as well as on the muscles data set, using the "geomorph" library (Adams et al., 2013) in R (Hornik, 2015). The higher the K-value is, the stronger the phylogenetic signal. A K-value of one corresponds to character evolution under Brownian motion. A K-value greater than one indicates a strong phylogenetic signal, which means that traits are conserved within the phylogeny. Conversely, a K-value close to zero means that phylogenetic signal is weak.

Study of the Skull Shape Variation Attributable to Muscles Data Using Linear Regression and Phylogenetic Regression

A linear regression and a regression in a phylogenetic context under a Brownian-motion model of evolution were performed in order to assess the impact of each muscle ($\log_{10}$ of PCSA and volume of each muscles) on the Procrustes coordinates as well as on the first three principal components of each bone of the skull (cranium and mandible). Both regressions were performed using respectively the "ProcD.lm" and the "procD.pgls" functions that are available in the 'Geomorph' (Adams et al., 2013) library in R (Hornik, 2015).

Study of the Co-Variation of Each Bone of the Skull and Muscle Data Using Two-Block Partial Least Squares and Phylogenetic Two-Block Partial Least Squares

To quantify co-variation between each of bone of the skull (cranium and mandible) and the muscles of the head (PCSA of all the mandibular adductors, volume of all the mandibular adductors, PCSA of the masseter group (SM + DM + ZM), volume of the masseter group (SM + DM + ZM), PCSA of the temporalis group (ST + DT + ZT), volume of the temporalis group (ST + DT + ZT)) we performed a two-block partial least squares (2B-PLS) approach (Rohlf and Corti, 2000) implemented in the library Geomorph (Adams et al., 2013) in R (Hornik, 2015).This method allows us to study co-variation between cranial and mandible shape and the volume and PCSA of the jaw muscles. A covariance matrix is calculated from two blocks representing the variation of the two objects (all the muscles (PCSA)—cranial shape, all the muscles muscles (Volume)—cranial shape; all the muscles muscles (PCSA)—mandibular shape, muscles (Volume)—mandibular shape). Two-block P analyses allow us to explore the patterns of co-variation by a reduction of dimensionality of the data, generating axes that explain the covariance between the shape and the support use. The PLS coefficient was calculated using the function "pls2b" in R (Hornik, 2015) using the Morpho library (Schlager, 2013) following the method PLS (Bookstein et al., 2003). This function uses 3D landmark data after superimposition and performs an analysis which is referred to as singular warp analysis (Bookstein et al., 2003). A significance test is obtained by 1,000 permutations of the landmarks in one block relative to those of the muscle data in the other. Then a sampling distribution of coefficients is obtained by resampling. The P_{95}-value is calculated by comparison of the observed PLS coefficient to those obtained after resampling. The significance of each linear combination is assessed by comparing the singular value (PLS coefficient) to those obtained from permuted blocks. If the PLS coefficient was higher than those obtained from permutated blocks, then its associated P_{95}-value is considered as significant.

As species share some part of their evolutionary history, they cannot be treated as independent data points. Thus, we also conducted these analyses in a phylogenetic framework (Felsenstein, 1985; Harvey and Pagel, 1991) using the phylogeny described earlier. We use the "phylo.integration" function (Adams et al., 2014) in R using the Geomorph library (Adams et al., 2013). This function allows us to quantify the degree of co-variation between the mean shape of each species for each bone and the muscles dataset while accounting for phylogeny using a partial generalized least squares algorithm under a Brownian motion model of evolution (Adams et al., 2014). A matrix of evolutionary covariance is obtained on which the "SVD" is performed. It consists of the eigen-decomposition of this phylogenetic covariance matrix. After this step evolutionary PLS scores are calculated from the two blocks of phylogenetically corrected data and the evolutionary correlation between the two blocks of the PLS scores (r_{PLS}) is evaluated. PLS correlation significance is assessed using phylogenetic permutation, where the shape or the muscle data for all species for one block are permutated on the tips of the phylogeny. The derived correlation scores are obtained from the permutated datasets and can be compared with the observed value.

RESULTS

Phylogenetic Signal

The results of the multivariate K-statistic calculated on the shape data are significant for the cranium ($K_{mult} = 0.58$, $P_{rand} = 0.001$) and the mandible ($K_{mult} = 0.96$, $P_{rand} = 0.001$). There is also a phylogenetic signal for muscle volume (All adductors: $K_{mult} = 0.68$, $P_{rand} = 0.004$; Masseter group: $K_{mult} = 0.69$, $P_{rand} = 0.003$; Temporal group: $K_{mult} = 0.65$, $P_{rand} = 0.005$) and PCSA data (All adductors: $K_{mult} = 0.64$, $P_{rand} = 0.003$; Masseter group: $K_{mult} = 0.68$, $P_{rand} = 0.003$; Temporal group: $K_{mult} = 0.61$, $P_{rand} = 0.004$). These results show significant phylogenetic signal in the shape of each bone of the skull and for muscle volume and PCSA. Closely related species

TABLE 4. Results of the regression analysis comparing the shape of each bone of the skull against the $\log_{10}$ of the PCSA of each muscles

		Regression						Phylogenetic regression					
		PC1		PC2		PC3		PC1		PC2		PC3	
Bone	PCSA	R^2	*P*	R^2	*P*	R^2	*P*	R^2	*P*	R^2	*P*	R^2	*P*
Cranium	DM	0.006	0.7	**0.74**	**0.001**	0.01	0.7	0.02	0.3	**0.48**	**0.001**	0.02	0.8
	DT	0.01	0.6	**0.55**	**0.001**	0.08	0.2	8E-04	0.9	**0.38**	**0.004**	0.008	0.7
	MP	0.001	0.8	**0.7**	**0.001**	0.05	0.34	0.03	0.4	**0.46**	**0.001**	0.02	0.5
	SM	0.009	0.6	**0.58**	**0.001**	0.1	0.18	0.01	0.6	**0.41**	**0.002**	0.01	0.6
	ST	0.002	0.8	**0.55**	**0.001**	0.07	0.26	0.009	0.6	**0.42**	**0.001**	0.006	0.7
	ZM	0.01	0.6	**0.6**	**0.001**	0.06	0.31	0.008	0.6	**0.33**	**0.002**	0.02	0.4
	ZT	0.000004	0.9	**0.6**	**0.001**	0.05	0.34	0.003	0.7	**0.33**	**0.003**	0.006	0.7
	Sum	0.0009	0.8	**0.6**	**0.001**	0.07	0.27	0.01	0.6	**0.45**	**0.001**	0.011	0.6
Mandible	DM	0.17	0.06	0.01	0.6	0.13	0.12	0.07	0.1	0.001	0.8	0.001	0.8
	DT	0.04	0.39	2E-04	0.9	0.17	0.06	0.01	0.61	0.01	0.6	0.01	0.7
	MP	0.16	0.08	0.04	0.39	0.12	0.12	0.07	0.22	0.004	0.8	0.001	0.8
	SM	0.04	0.36	0.001	0.8	0.09	0.2	0.02	0.49	0.01	0.6	0.002	0.8
	ST	0.13	0.12	0.002	0.8	0.05	0.34	0.03	0.36	0.007	0.7	0.001	0.8
	ZM	0.08	0.22	0.02	0.4	**0.26**	**0.02**	0.05	0.27	2E-04	0.9	0.005	0.7
	ZT	0.14	0.1	0.006	0.7	**0.23**	**0.03**	0.03	0.4	0.01	0.6	0.007	0.7
	Sum	0.1	0.18	0.008	0.68	0.14	0.1	0.04	0.32	0.04	0.77	2E-04	0.9

R^2 indicates the correlation between the two variables of interest based on regressions. Significant correlations are indicated in bold.

thus have similar shapes and similar muscle volumes and PCSAs.

Quantification of the Procrustes Variance (Disparity) of the Cranial and Mandibular Shape

The result of the calculation of the procrustes variance show that the mandible (Procrustes variance = 0.016) have a higher disparity than the cranium (Procrustes variance = 0.011).

Study of the Skull Shape Variation Attributable to Muscles Data Using Linear Regression and a Phylogenetic Regression

Results of the regression analyses show a significant effect of the muscle PCSA on cranial shape for each of the muscles (Supporting Information Table S2). Results of the phylogenetic regressions show a significant effect of the muscle PCSA on cranial shape only for the deep masseter, the medial pterygoid, the superficial temporal, and the sum of all PCSAs (Supporting Information Table S2). Concerning the regressions of the volume of each muscle on cranial shape, the results indicate a significant correlation between cranial shape and the volume of all muscles (Supporting Information Table S3). When phylogeny is taken into account, the results indicate a significant correlation between cranial shape and the volume of the deep masseter, the medial pterygoid, the superficial masseter, the superficial temporalis, the temporalis pars suprazygomatica and the sum of all muscle volumes (Supporting Information Table S3). Results of the non-phylogenetic regression and phylogenetic regression are also significant for the impact of muscle PCSA and volume on the second PC axes describing cranial shape (accounting for >17% of the variance) (Tables 4 and 5).

Results of the non-phylogenetic regression and phylogenetic regression analysis comparing the shape of the mandible and muscle PCSA and volume of the muscles show no correlations (Supporting Information Tables S2 and S3). When looking at the results of the regressions performed on the PC scores, a significant effect of the PCSA on the third PC axis describing mandibular shape (accounting for >7% of the variance) was observed for only the temporalis pars suprazygomatica and the zygomatico-mandibularis (Table 4). The result is similar to the previous one for the volume of the muscle with one additional muscle, the deep temporalis, which impacts the third PC axis describing mandibular shape. None of the results are significant when phylogeny is taken into account (Table 5).

Study of the Co-Variation of the Cranium and Mandible and Muscle Data Using 2B-PLS and Phylogenetic 2B-PLS

Co-variation between cranial shape and the masticatory muscles (PCSA and volume). The co-variation observed between cranial shape and the masticatory muscles is highly significant (PCSA of the muscles: $r_{PLS} = 0.\ 9$, $P_{rand} = 0.001$, Table 6 and Fig. 3; Volume of the muscles: $r_{PLS} = 0.\ 9$, $P_{rand} = 0.001$, Table 7 and Fig. 4). When exploring the co-variation between cranial shape and the masseter and temporalis group similar results are observed (PCSA of the masseter group: $r_{PLS} = 0.\ 9$, $P_{rand} = 0.001$, Table 6; PCSA of the temporalis group: $r_{PLS} = 0.\ 89$, $P_{rand} = 0.002$, Table 6; volume of the masseter group: $r_{PLS} = 0.\ 9$, $P_{rand} = 0.001$, Table 7; volume of the temporalis group: $r_{PLS} = 0.\ 9$, $P_{rand} = 0.001$, Table 7). Because results of the co-variance analyses with muscle volume and PCSA are nearly identical we will here describe only the results for the co-variation between the cranial shape and the PCSA of all the masticatory muscles. The scatterplot of the 2B-PLS (Fig. 3) shows that species that occupy the

TABLE 5. Results of the regression analysis comparing the shape of each bone of the skull against the log_{10} of the volume of each muscles

		Regression						Phylogenetic regression					
		PC1		PC2		PC3		PC1		PC2		PC3	
Bone	Volume	R^2	*P*	R^2	*P*	R^2	*P*	R^2	*P*	R^2	*P*	R^2	*P*
Cranium	DM	6E-06	0.9	**0.73**	**0.001**	0.03	0.4	0.009	0.6	**0.45**	**0.001**	0.0001	0.9
	DT	0.01	0.6	**0.57**	**0.001**	0.05	0.3	0.003	0.82	**0.37**	**0.003**	0.0003	0.9
	MP	0.007	0.7	**0.67**	**0.001**	0.06	0.3	3E-04	0.9	**0.49**	**0.001**	0.006	0.6
	SM	0.03	0.4	**0.56**	**0.001**	0.07	0.2	0.002	0.7	**0.39**	**0.002**	0.0001	0.9
	ST	0.004	0.7	**0.59**	**0.001**	0.04	0.4	0.002	0.8	**0.42**	**0.002**	0.0002	0.9
	ZM	0.01	0.5	**0.65**	**0.001**	0.05	0.3	4E-05	0.9	**0.33**	**0.003**	0.007	0.6
	ZT	1E-06	0.9	**0.7**	**0.001**	0.03	0.4	6E-04	0.8	**0.51**	**0.001**	4E-05	0.9
	Sum	0.008	0.7	**0.64**	**0.001**	0.05	0.35	7E-04	0.89	**0.44**	**0.002**	0.0004	0.9
Mandible	DM	0.12	0.12	0.01	0.6	0.17	0.07	0.06	0.19	0.003	0.8	8E-05	0.9
	DT	0.03	0.4	0.001	0.8	**0.21**	**0.04**	0.006	0.7	0.02	0.4	0.03	0.4
	MP	0.08	0.2	0.03	0.4	0.18	0.06	0.05	0.17	9E-05	0.9	0.004	0.7
	SM	0.02	0.5	0.005	0.7	0.13	0.12	0.02	0.4	0.01	0.55	6E-05	0.9
	ST	0.05	0.3	8E-04	0.8	0.11	0.15	0.01	0.6	0.02	0.4	0.005	0.7
	ZM	0.07	0.25	0.01	0.6	**0.3**	**0.01**	0.03	0.36	0.006	0.7	0.02	0.4
	ZT	0.12	0.1	0.002	0.8	**0.23**	**0.03**	0.03	0.28	0.01	0.6	0.03	0.3
	Sum	0.06	0.29	0.001	0.8	0.18	0.06	0.02	0.43	0.01	0.5	0.01	0.6

R^2 indicates the correlation between the two variables of interest based on regressions. Significant correlations are indicated in bold.

TABLE 6. Results of the co-variation analysis comparing the shape of each bone of the skull against the log_{10} of all PCSA of the muscles, the log_{10} of PCSA of the masseter group and PCSA of the log_{10} of the zygomatic group

		2B-PLS		Phylogenetic 2B-PLS	
Shape	Muscles (PCSA)	r-PLS	P-value	r-PLS	P-value
Cranium	ALL muscles	**0.9**	**0.001**	**0.79**	**0.05**
	Masseter group	**0.9**	**0.001**	0.78	0.07
	Temporalis group	**0.89**	**0.002**	0.79	0.06
Mandible	ALL muscles	0.48	0.2	0.4	0.7
	Masseter group	0.48	0.2	0.4	0.8
	Temporalis group	0.46	0.29	0.43	0.7

R-PLS indicates the coefficient of co-variation between the two variables of interest based on 2B-PLS and phylogenetic 2B-PLS. Significant results are indicated in bold.

positive part of the scatterplot are mainly insectivorous with some frugivores whereas species that occupy the negative part of the scatterplot are mainly hard-object (the aye-aye) and leaf-eaters (sifakas and bamboo lemurs), along with the majority of the frugivores. The main muscles that co-vary with cranial shape are the deep masseter, the zygomatico-mandibularis, the temporalis pars suprazygomatica, and the medial pterygoid. The positive part of the scatterplot corresponds to the species with a low PCSA of these muscles and a cranium with a relatively thin postorbital bar and zygomatic arch, an orbito-temporal fossa that is relatively small, a round braincase with a temporal line which is lower down on the side of the braincase, a relatively elongated snout, and a relatively wide and laterally open pterygoid region. In contrast, the negative part of the scatterplot corresponds to the species with a high PCSA and a cranium with a relatively robust postorbital bar and zygomatic arch, an orbito-temporal fossa that is relatively well developed, an oval-shaped braincase with a temporal line that is close to the midline, a relatively short snout, and relatively narrow pterygoid plates.

Phylogenetic co-variation between the cranial shape and the masticatory muscles taking (PCSA and volume). The results of the phylogenetic 2B-PLS show a tendency for significant co-variation between cranial shape and the PCSA of the muscles ($r_{PLS} = 0.79$, $P_{rand} = 0.05$, Table 6 and Fig. 5). Whereas the result of the phylogenetic 2B-PLS is still significant between the cranial shape and the volume of the muscles ($r_{PLS} = 0.\ 8$, $P_{rand} = 0.04$, Table 7 and Fig. 6). When exploring the phylogenetic co-variation between cranial shape and the masseter and temporalis group, our results show again a tendency to be significant (PCSA of the masseter group: $r_{PLS} = 0.\ 78$, $P_{rand} = 0.07$, Table 6; PCSA of the temporalis group: $r_{PLS} = 0.\ 79$, $P_{rand} = 0.06$, Table 6; volume of the masseter group: $r_{PLS} = 0.\ 79$, $P_{rand} = 0.06$, Table 7). Only the phylogenetic co-variation between cranial shape and the volume of the temporalis muscle group is significant ($r_{PLS} = 0.\ 9$, $P_{rand} = 0.001$, Table 7). The scatterplots of the phylogenetic co-variation between cranial shape and the masticatory muscles (PCSA and volume as well as for each group of muscles) are very similar. However, the loading of the muscles that co-vary with cranial shape is different when the two muscle dimensions (PCSA and volume) are considered. The scatterplot describing phylogenetic co-variation tends to separate the insectivorous and some of the frugivorous species (*Eulemur*, *Otolemur*, and *Varecia*) at the positive part of the axis from the other frugivores (*Cheirogaleus*, *Perodicticus*, and *Microcebus*), hard-object and leaf-eaters species at the negative part of the axis. It exacerbates the difference between two sister taxa: *Galago demidoff* in the positive part of the axis and *Otolemur crassicaudatus* in the negative part. These species thus appear to differ in the co-evolution of

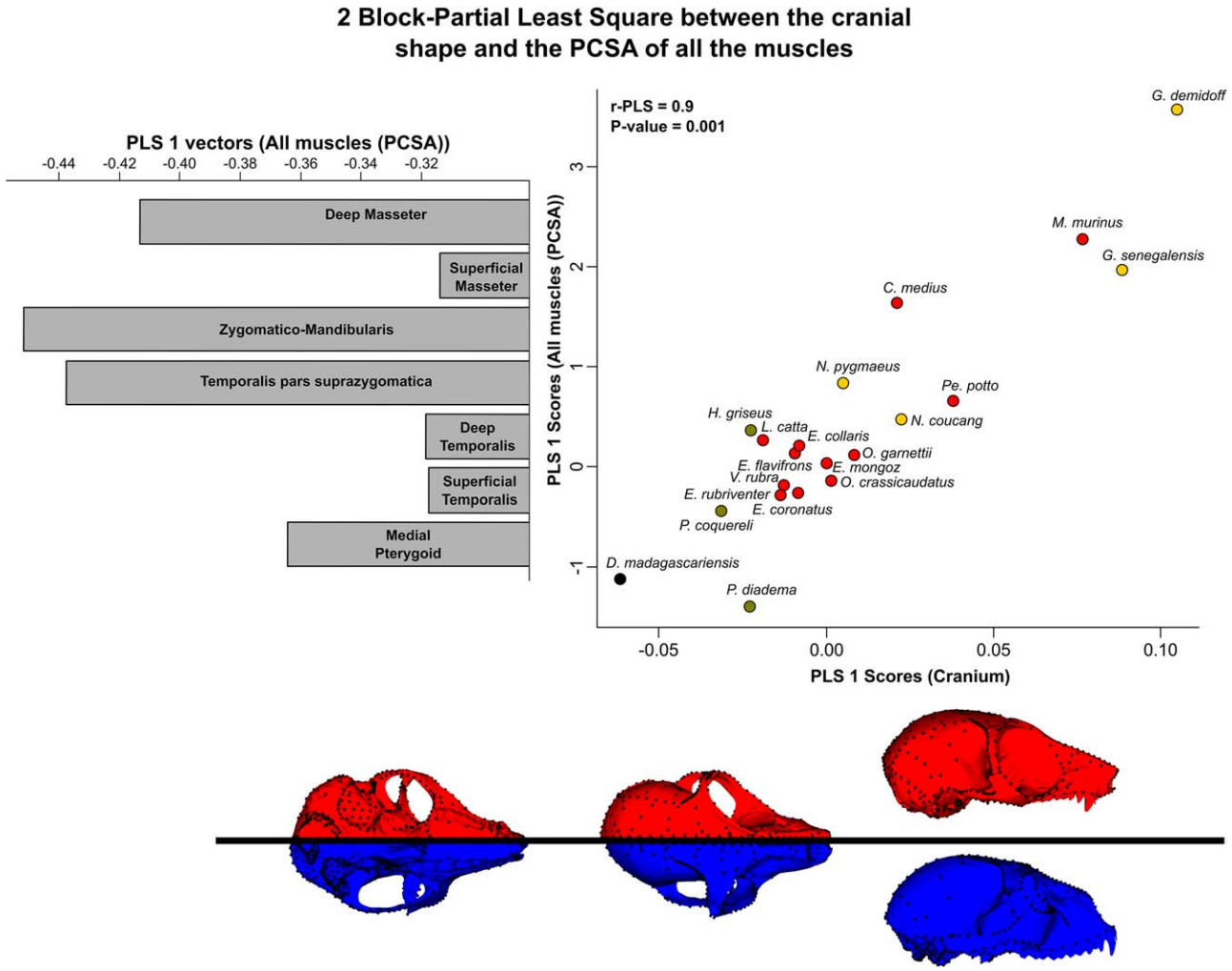

Fig. 3. Results of the 2B-PLS between the cranial shape and the PCSA of the masticatory muscles. Scatter plot of the first PLS axis describing the co-variation between cranial shape and the PCSA of the masticatory muscles. Color code of the points in the scatterplot represents the diet of each species with: red points representing frugivores, green khaki points representing folivores, yellow points represent insectivores, and black point representing the aye-aye. Cranial shapes associated with each minimum and maximum of co-variation are illustrated in blue and red, respectively, at the bottom of the scatter plot (from left to right side: ventral view, dorsal view and lateral view). Muscle loadings associated with the cranial shape co-variation are represented by the histogram at the left side of the scatterplot.

TABLE 7. Results of the co-variation analysis comparing the shape of each bone of the skull against the $\log_{10}$ of all volume of the muscles, the $\log_{10}$ of volume of the masseter group and volume of the $\log_{10}$ of the zygomatic group

Shape	Muscles (volume)	2B-PLS		Phylogenetic 2B-PLS	
		r-PLS	P-value	r-PLS	P-value
CRANIUM	ALL muscles	**0.9**	**0.001**	**0.8**	**0.04**
	Masseter group	**0.9**	**0.001**	0.79	0.06
	Temporalis group	**0.9**	**0.001**	**0.8**	**0.04**
MANDIBLE	ALL muscles	0.45	0.3	0.4	0.75
	Masseter group	0.46	0.28	0.39	0.84
	Temporalis group	0.33	0.44	0.49	0.44

R-PLS indicates the coefficient of co-variation between the two variables of interest based on 2B-PLS and phylogenetic 2B-PLS. Significant results are indicated in bold.

their cranial shape and masticatory muscles. For the co-variation between the PCSA of the muscles and cranial shape, the main muscles which impact the cranial shape are, by order of importance: the deep masseter, the medial pterygoid, the zygomatico-mandibularis, the temporalis pars suprazygomatica, the superficial temporalis, and the superficial masseter. Species at the negative part of the axis of the scatterplot are associated with a high PCSA of these muscles and a cranium with a relatively broad postorbital bar and zygomatic arch, an orbito-temporal fossa that is relatively big, an oval-shaped braincase with a temporal line which is close to the midline, and relatively wide and laterally flaring pterygoid plates (Fig. 5). Whereas species at the positive side of the axis of the scatterplot are associated with a low PCSA and a cranium with a relatively thin postorbital bar and zygomatic arch, an orbito-temporal fossa that is relatively small, a rounder braincase with a temporal line which is lower down on the side of the braincase, and relatively narrow pterygoid plates (Fig. 5).

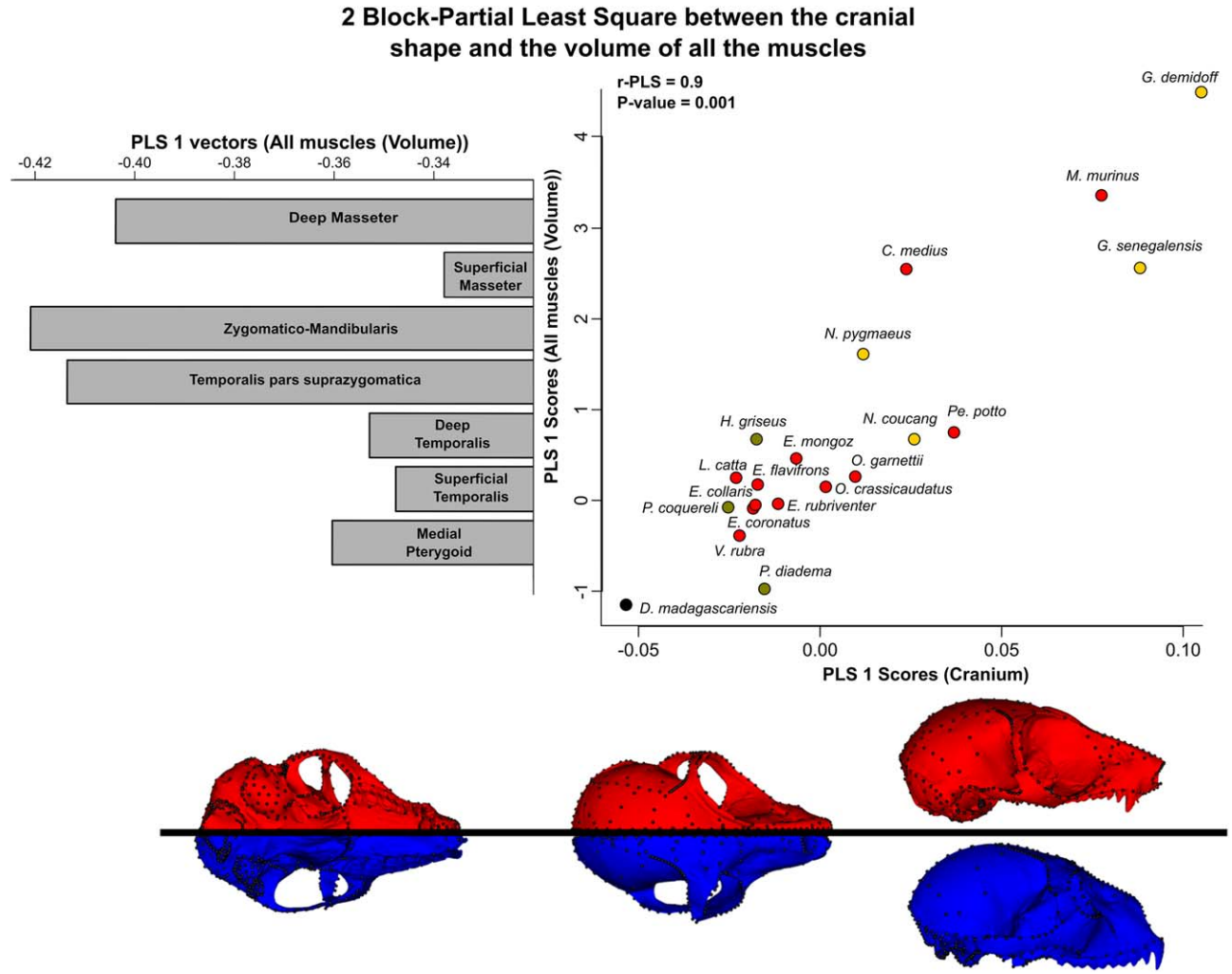

Fig. 4. Results of the 2B-PLS between the cranial shape and the volume of the masticatory muscles. Scatter plot of the first PLS axis describing the shape co-variation between cranial shape and the volume of the masticatory muscles. Color code of the points in the scatterplot represents the diet of each species with: red points representing frugivores, green khaki points representing folivores, yellow points represent insectivores, and black point representing the aye-aye. Cranial shapes associated with each minimum and maximum of co-variation are illustrated in blue and red, respectively, at the bottom of the scatter plot (from left to right side: ventral view, dorsal view and lateral view). Muscle loadings associated with the cranial shape co-variation are represented by the histogram at the left side of the scatterplot.

For the phylogenetic co-variation between the volume of the muscles and the cranial shape, the main muscles that co-vary with cranial shape are, by order of importance: the deep masseter, the superficial temporalis, the temporalis pars suprazygomatica, the deep temporalis and the superficial masseter. Species at the negative part of the axis of the scatterplot are associated with a high volume of these muscles and display a cranium with a relatively broad postorbital bar and zygomatic arch, an orbito-temporal fossa that is relatively big, an oval-shaped braincase with a temporal line close to the midline, and relatively wide and laterally flaring pterygoid plates (Fig. 6).

Co-variation between the mandibular shape and the masticatory muscles (PCSA and volume). There is no significant co-variation between the mandibular shape and the PCSA (Table 6) and volume (Table 7) of the masticatory muscles for the first PLS axis (accounting for 73.8% of the covariance for the PCSA and 73.7% for the volume). The results are still not significant when accounting for the phylogenetic effect (Table 6 and 7). However, the co-variations between mandibular shape and the PCSA of the masticatory muscles shows a tendency to be significant for the third axis of the PLS accounting for 7.4% of the covariance ($r_{PLS} = 0.4$, $P_{rand} = 0.055$; Fig. 7 and Table 6). The scatterplot for these analyses shows a difference between a hard-object eater species (*Daubentonia madagascariensis*) on the negative side of the axis and the folivorous species (*Hapalemur* and *Propithecus*). All the frugivorous and insectivorous species cluster in a vertical line in the middle of the scatterplot. The differences in co-variation of mandibular shape and the masticatory muscles can be explained by a strong deep temporalis, superficial masseter and superficial temporalis

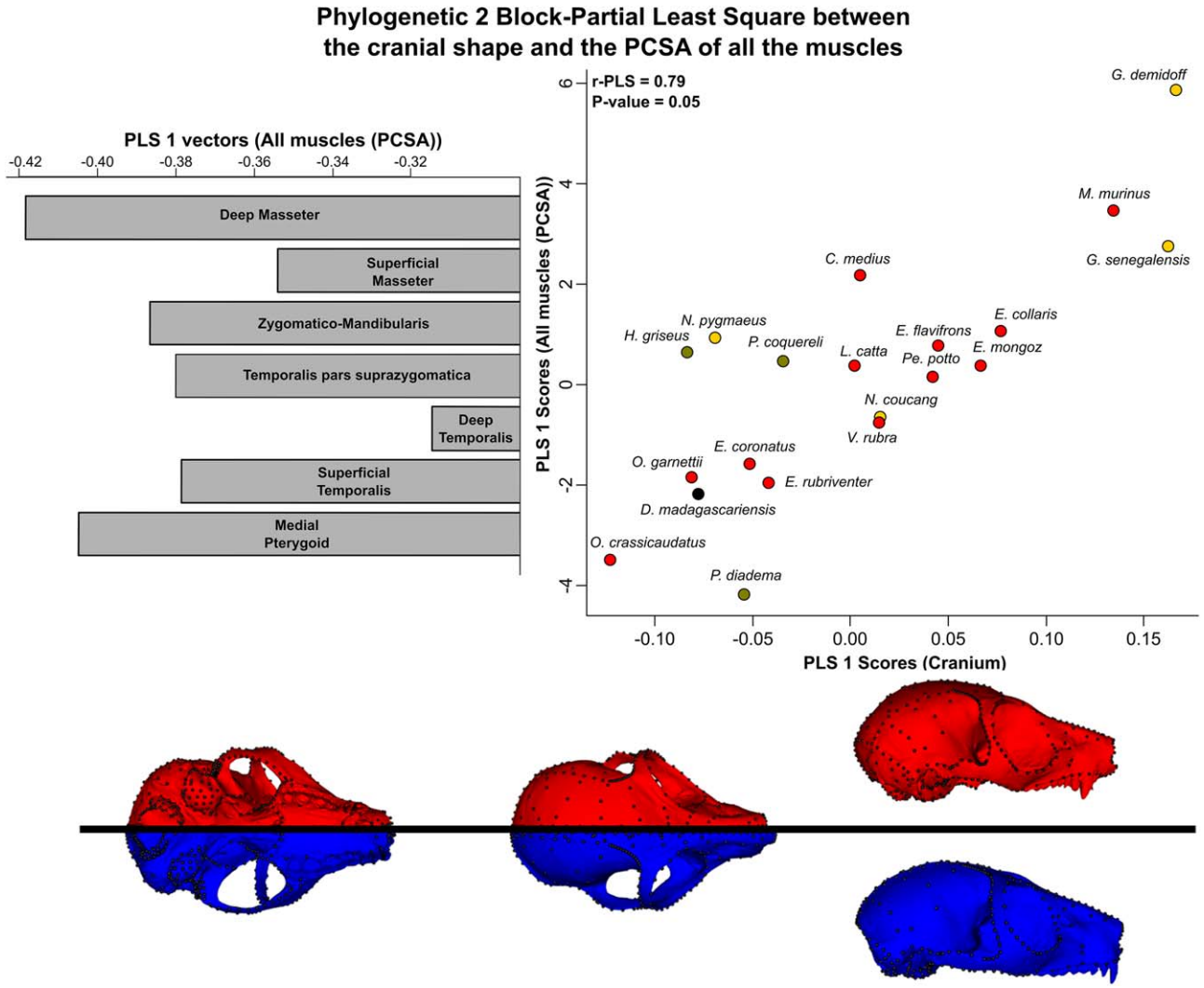

Fig. 5. Results of the phylogenetic 2B-PLS between the cranial shape and the PCSA of the masticatory muscles. Scatter plot of the first PLS axis describing the shape co-variation between cranial shape and the PCSA of the masticatory muscles. Color code of the points in the scatterplot represents the diet of each species with: red points representing frugivores, green khaki points representing folivores, yellow points represent insectivores, and black point representing the aye-aye. Cranial shapes associated with each minimum and maximum of co-variation are illustrated in blue and red, respectively, at the bottom of the scatter plot (from left to right side: ventral view, dorsal view and lateral view). Muscle loadings associated with the cranial shape co-variation are represented by the histogram at the left side of the scatterplot.

associated with a less well-developed coronoid and angular process, a condyle that is very low and a robust ramus for species along the negative part of the axis. In contrast, the co-variation in the positive part of the axis can be explained by a strong zygomatico-mandibularis and medial pterygoid in association with a well-developed coronoid and angular process, a condyle that is really high and a thinner ramus of the mandible (Fig. 7).

The co-variations are significant between mandibular shape and the volume of the masticatory muscles for the third and fourth PLS axes accounting respectively for 7.6% and 4.7% of the overall co-variation (Third PLS axis: $r_{PLS} = 0.45$, $P_{rand} = 0.01$; Fourth PLS axis: $r_{PLS} = 0.59$, $P_{rand} = 0.003$; Figs. (8 and 9) and Table 7). The scatterplot of the third axis tends to differentiate all the frugivorous species (e.g. *Eulemur* and *Varecia*) at the negative side of the axis from the aye-aye (*D. madagascariensis*). This distribution of species can be explained on the negative side of the axis by, a large superficial masseter, zygomatico-mandibularis and medial pterygoid muscles associated with a mandible that is relatively gracile, with a coronoid process that is vertically oriented and a ramus that is elongated. In contrast, species on the positive side have a large deep masseter, temporalis pars suprazygomatica, and a superficial temporalis associated with a robust mandibular shape, with a wide angular process, an elongated coronoid process oriented backward, and a ramus that is relatively short (Fig. 8).

The fourth axis of co-variation between the volume and mandibular shape (Fig. 9) shows a distribution that

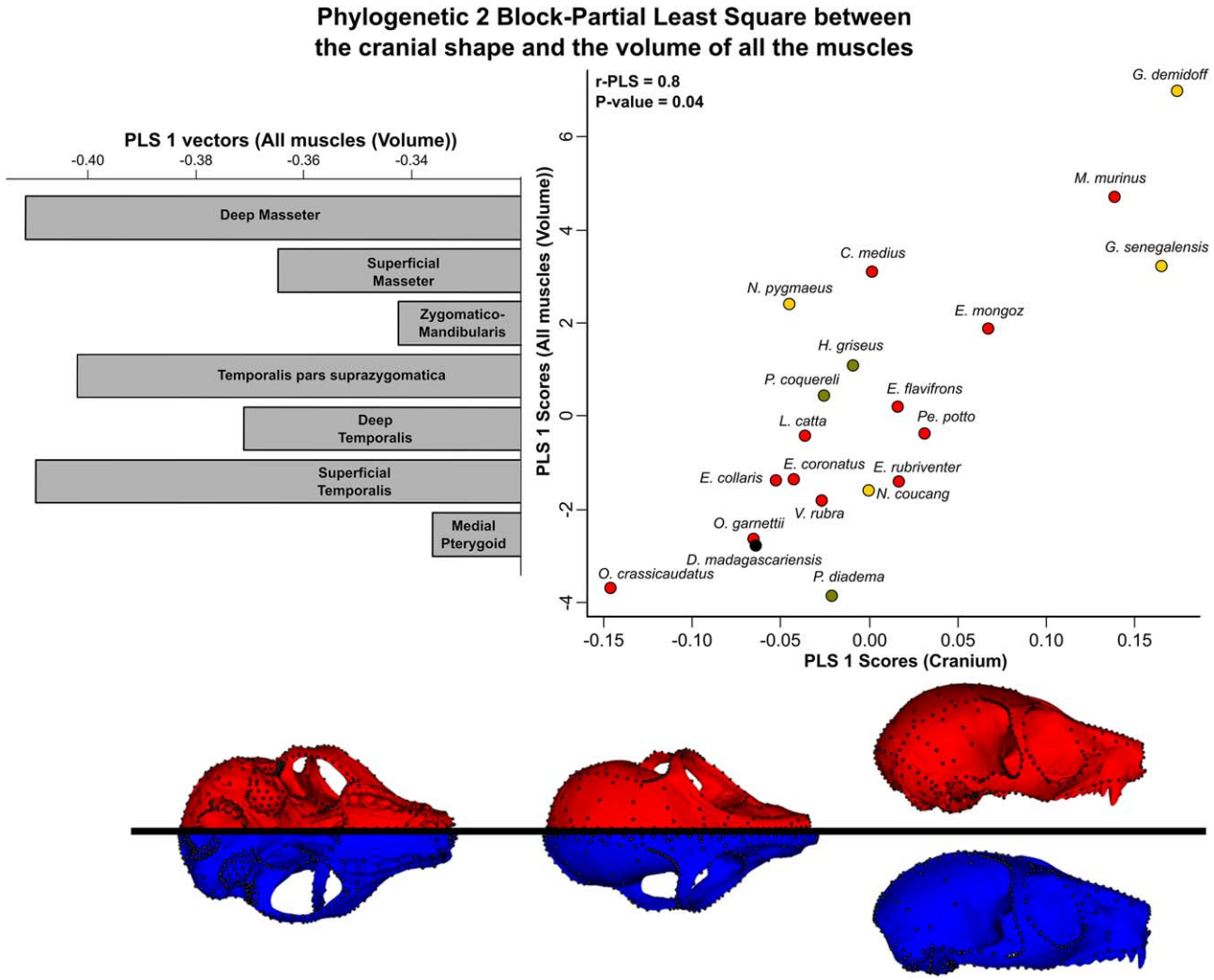

Fig. 6. Results of the phylogenetic 2B-PLS between the cranial shape and the volume of the masticatory muscles. Scatter plot of the first PLS axis describing the shape co-variation between cranial shape and the volume of the masticatory muscles. Color code of the points in the scatterplot represents the diet of each species with: red points representing frugivores, green khaki points representing folivores, yellow points represent insectivores, and black point representing the aye-aye. Cranial shapes associated with each minimum and maximum of co-variation are illustrated in blue and red, respectively, at the bottom of the scatter plot (from left to right side: ventral view, dorsal view and lateral view). Muscle loadings associated with the cranial shape co-variation are represented by the histogram at the left side of the scatterplot.

tends to differentiate both greater bushbabies (*Otolemur*) on the negative part of the axis from the aye-aye (*D. madagascariensis*) on the positive part of the axis. Species at the negative side of the axis display a large superficial masseter, medial pterygoid and superficial temporalis in association with well-developed angular and coronoid processes and a thinner ramus of the mandible. In contrast, species at the positive side of the axis have a large zygomatico-mandibularis and temporalis pars suprazygomatica in association with a less developed angular and coronoid process, a more developed articulation with the cranium, and a ramus of the mandible that is more robust (Fig. 9).

Evolutionary co-variation between mandibular shape and volume of the masticatory muscles. When the phylogeny is taken into account, there is no significant co-variation between the shape of the mandible and the masticatory muscles (Table 6 and 7).

DISCUSSION

Phylogenetic Signal

Our results show that there is a moderately high phylogenetic signal for each bone and in the muscles of the masticatory system. Species that are closely related tend to have a similar skull shape and size of the masticatory muscles. Similar results were already found for the skull shape (Baab et al., 2014; Meloro et al., 2015). However, our results differ from those found in the study of Perry et al. (2015) concerning the masticatory muscles. They found a low lambda values for most muscles indicating for little phylogenetic signal, whereas in our study, we found a moderately high signal using a generalized K statistic.

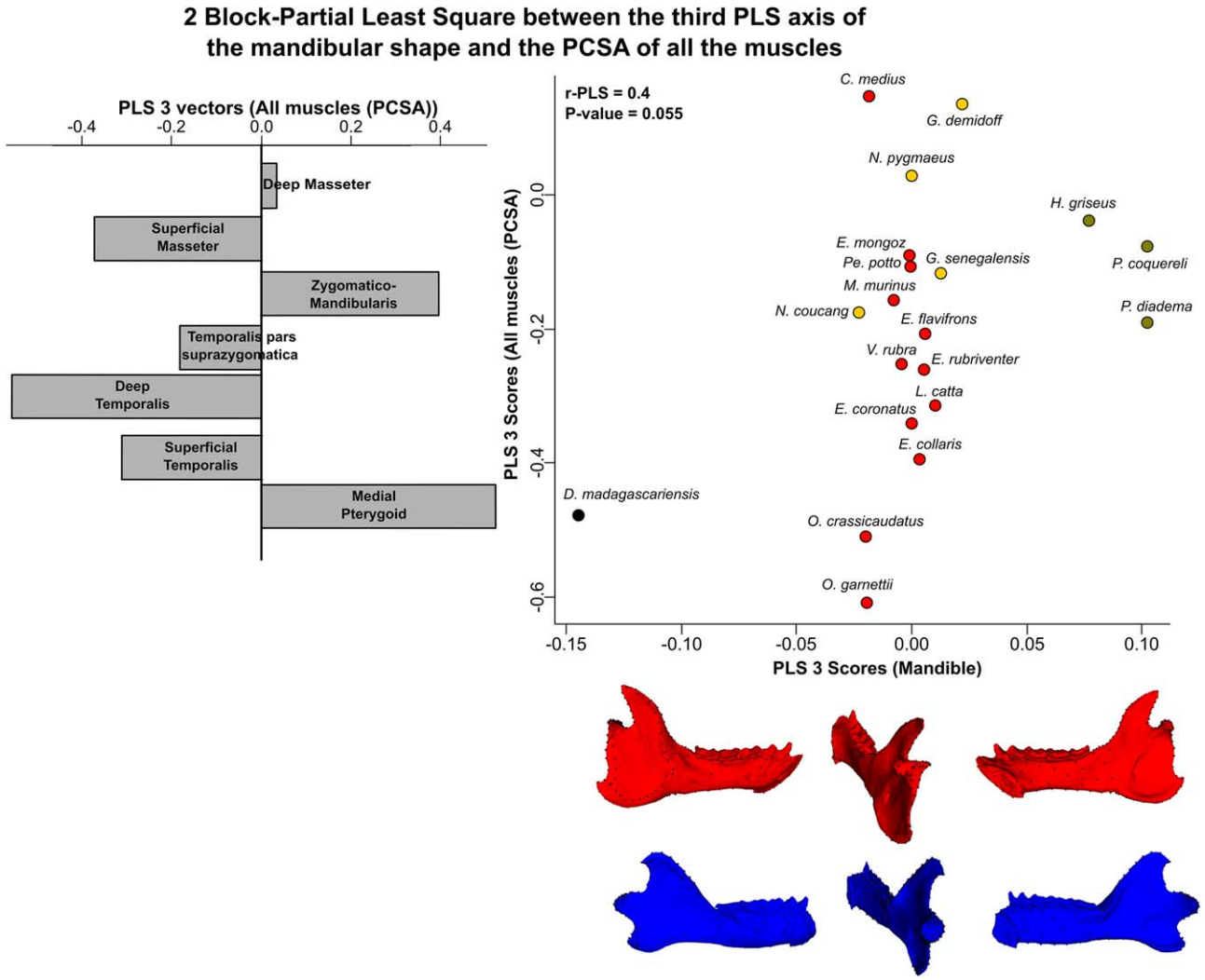

Fig. 7. Results of the 2B-PLS between the mandibular shape and the PCSA of the masticatory muscles. Scatter plot of the third PLS axis describing the shape co-variation between mandibular shape and the PCSA of the masticatory muscles. Color code of the points in the scatterplot represents the diet of each species with: red points representing frugivores, green khaki points representing folivores, yellow points represent insectivores, and black point representing the aye-aye. Mandibular shapes associated with each minimum and maximum of co-variation are illustrated in blue and red, respectively, at the bottom of the scatter plot (from left to right side: lateral view, superior view and medial view). Muscle loadings associated with the cranial shape co-variation are represented by the histogram at the left side of the scatterplot.

Impact of Masticatory Muscles on the Shape of Cranial Bones

Few studies have tried to assess the impact of the relationships between the masticatory muscles and the shape of the cranial bones (but see Cornette et al., 2013, 2015; Fabre et al., 2014a). However, this is an important step to understand the function of the musculoskeletal system (interaction between muscles and bones) and may help formulate hypotheses concerning the functional significance of certain morphological traits. In our study, the results of the regressions show that masticatory muscles highly impact the shape of the cranium but to a lesser degree the mandible.

The results of co-variation analyses also show similar trends with a strong co-variation between the masticatory muscles and the shape of the cranium and a lower co-variation between the masticatory muscles and the mandible. Our results for the cranium differ from those of the study of Toro-Ibacache et al. (2016). In their study, they found no co-variation between cranial shape and muscular CSA of the jaw muscles in humans. This difference can be due to the fact that CSA does not provide the same signal as the PCSA values calculated here, or maybe because something different happened during the evolution of the human masticatory system, the skull being strongly constrained by the large brain and sensory organs (Stedman et al., 2004; Oxnard, 2008). Several studies have shown that the masticatory muscles of humans are «reduced» compared with other primates (Lieberman et al., 2004; Oxnard, 2008; Wroe et al., 2010; Eng et al., 2013). This is possibly due to a lack of selection because of cooking (Stedman et al., 2004; Eng et al., 2013).

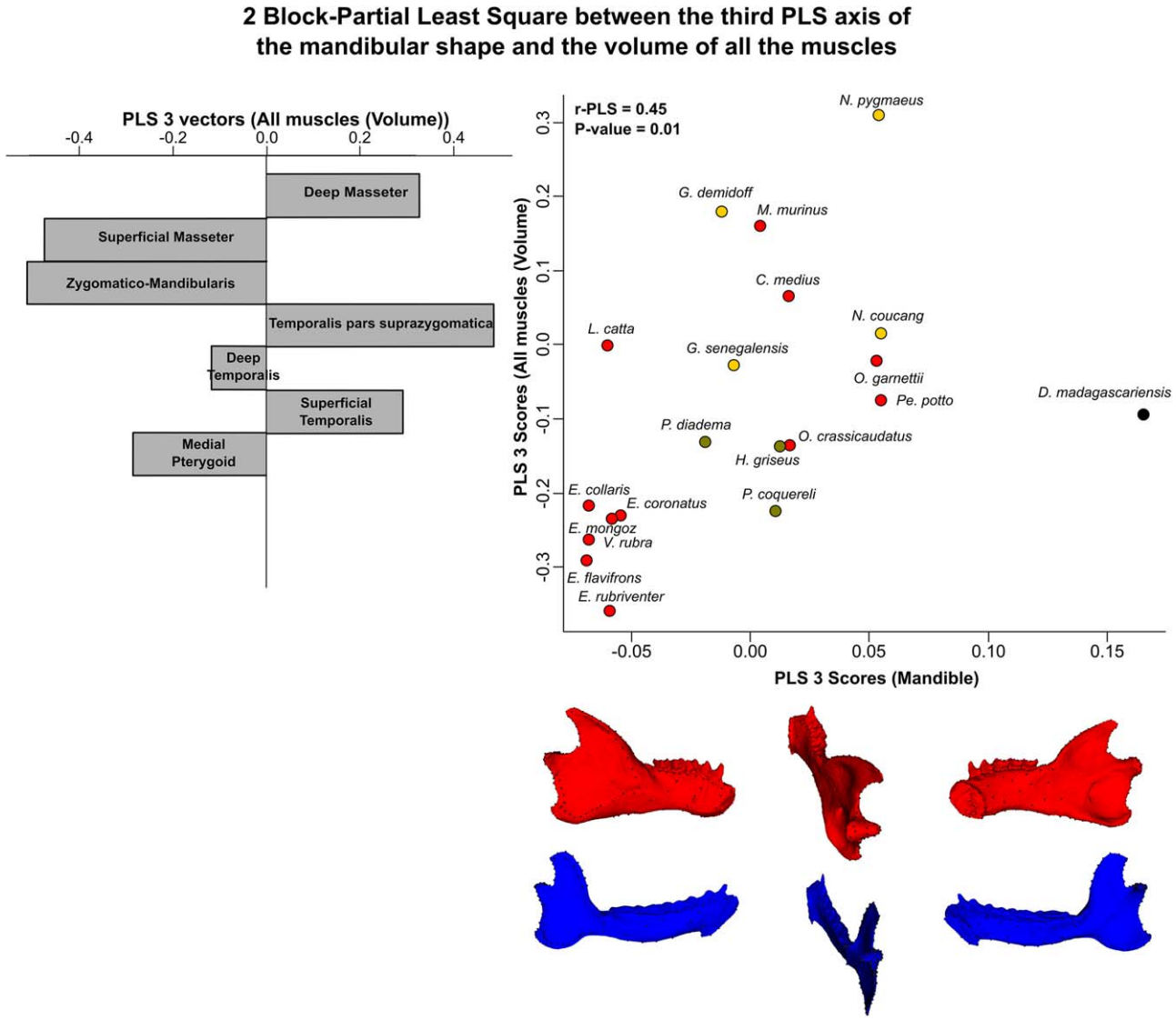

Fig. 8. Results of the 2B-PLS between the mandibular shape and the volume of the masticatory muscles. Scatter plot of the third PLS axis describing the shape co-variation between mandibular shape and the volume of the masticatory muscles. Color code of the points in the scatterplot represents the diet of each species with: red points representing frugivores, green khaki points representing folivores, yellow points represent insectivores, and black point representing the aye-aye. Mandibular shapes associated with each minimum and maximum of co-variation are illustrated in blue and red, respectively, at the bottom of the scatter plot (from left to right side: lateral view, superior view and medial view). Muscle loadings associated with the cranial shape co-variation are represented by the histogram at the left side of the scatterplot.

In our results, the main masticatory muscles that co-vary with cranial shape are the deep masseter, the zygomatico-mandibularis, and the temporalis pars suprazygomatica (Figs. 3 and 4). Shape changes are mainly located on the zygomatic arch, the orbito-temporal fossa, and the braincase and temporal line (Figs. 3 and 4). All these muscles attach to, or are influenced by, the zygomatic arch (Fig. 10 and Table 8). Their strong co-variations tend to confirm that when these muscles are strong (or bulky), the associated zygomatic arch is robust and vice versa. These muscles co-vary also with the orbito-temporal fossa and the shape of the braincase. Indeed, the temporalis pars suprazygomatica muscle takes its origin on the orbito-temporal fossa (medial and dorsal to the zygomatic arch), passes through the temporal fossa and inserts on the coronoid process of the mandible (Fig. 10 and Table 8). A stronger (or bulky) temporalis pars suprazygomatica muscle co-varies with a bigger and more elongated temporal fossa and a braincase with a wider area of insertion of the temporalis (Figs. 3 and 4). Concerning the zygomatico-mandibularis muscle, it originates from the inferior medial surfaces of the zygomatic arch and inserts into masseteric fossa and on the ascending ramus of the mandible (Fig. 10 and Table 8). A strong (or bulky) zygomatico-mandibularis co-varies with a bigger and more elongated temporal fossa (Fig. 10 and Table 8).

Nevertheless, when the phylogeny is taken into account, some differences can be observed. Indeed, it

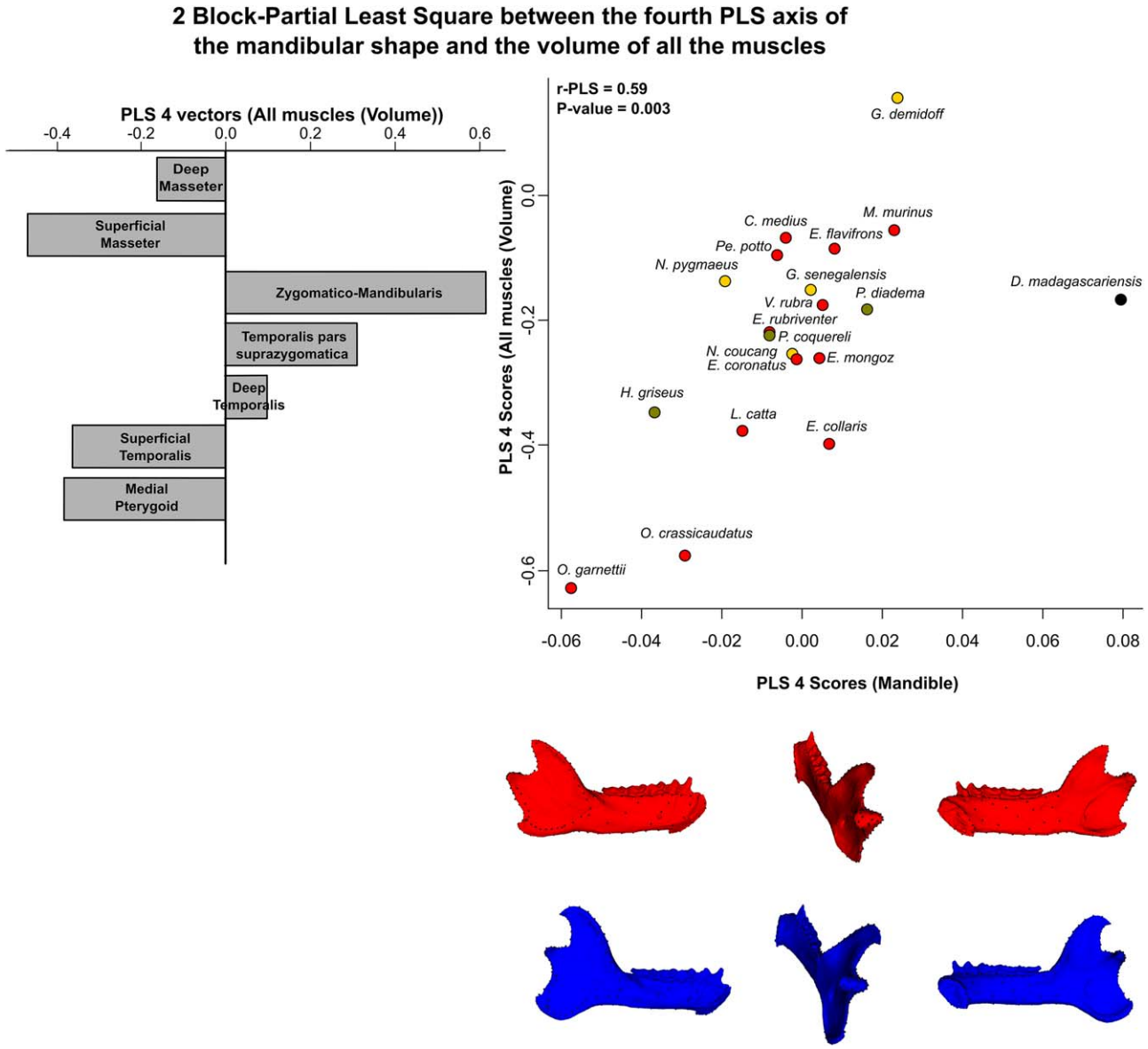

Fig. 9. Results of the 2B-PLS between the mandibular shape and the volume of the masticatory muscles. Scatter plot of the fourth PLS axis describing the shape co-variation between mandibular shape and the volume of the masticatory muscles. Color code of the points in the scatterplot represents the diet of each species with: red points representing frugivores, green khaki points representing folivores, yellow points represent insectivores, and black point representing the aye-aye. Mandibular shapes associated with each minimum and maximum of co-variation are illustrated in blue and red, respectively, at the bottom of the scatter plot (from left to right side: lateral view, superior view and medial view). Muscle loadings associated with the cranial shape co-variation are represented by the histogram at the left side of the scatterplot.

seems that two species of galagos that are closely related have a different co-evolution between the shape of their cranium and their masticatory muscles (Figs. 5 and 6). Whereas the dominant food source in *Eulemur*, *Varecia*, and *Otolemur* is fruit, a secondary component of the diet for the larger ones is leaves (gum in *Otolemur*). Thus, it seems that insect eaters (*Galago*, *Microcebus*) are differentiated from leaf or seed eaters (*Otolemur*, *Daubentonia*, *Propithecus*, *Hapalemur*) (Figs. 5 and 6). Fruit, as it is relatively easy to break down, seems not to have a strong impact on the morphology. Because larger primates tend to derive their protein from leavs and smaller ones derive their protein from insects (e.g. Kay, 1975; Kay and Sheine, 1979; Chivers et al., 1984; Kay et al., 2004), this could also be a size-related shape trend.

In both phylogenetic co-variations (PCSA and volume), there are some muscles in common that co-vary with the cranium: the deep masseter, the zygomatico-mandibularis, the temporalis pars suprazygomatica, and the superficial temporalis. The deep masseter is an important muscle for generating a transverse load, which is important during the processing of leaves. It attaches on the zygomatic arch and may explain the co-

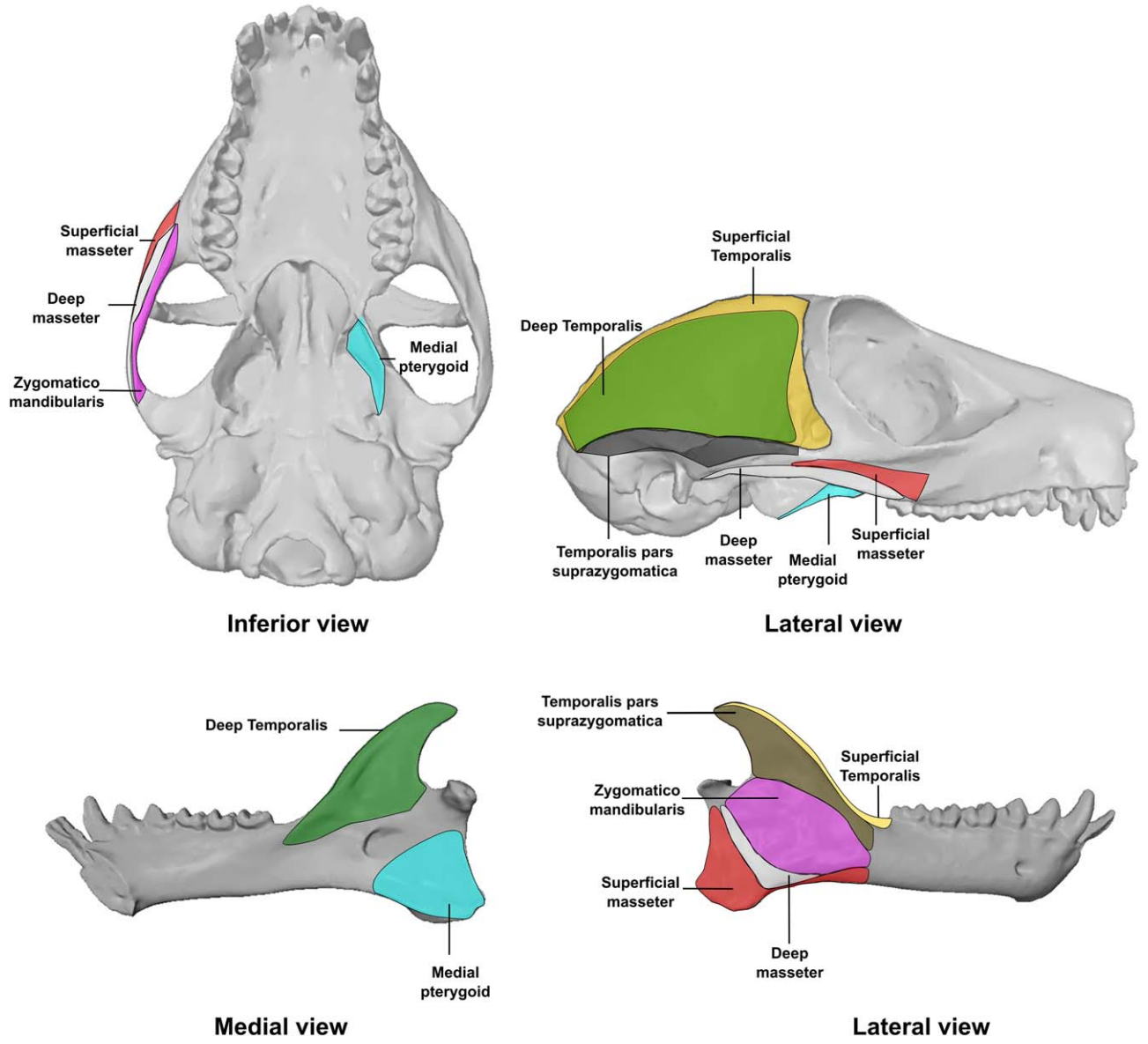

Fig. 10. Schematic figure illustrating the origins and insertions of muscles discussed in the manuscript. Definition of the muscle origins, insertions can be found in Table 8.

variation with a broad zygomatic arch and a wide temporal fossa. The temporalis pars suprazygomatica attaches on the lateral border of the braincase (Fig. 10 and Table 8), this muscle may play a role in the transition from opening to closing the jaw, but its function remains poorly known. In the phylogenetic co-variation results describing the relationship between the cranium and the PCSA of the muscles, the zygomatico-mandibularis and the medial pterygoid are well-developed in the insect and leaf eaters whereas in the co-variations between the cranium and muscle volume this is not the case. This may reflect the importance of these muscles when animals are processing leaves and may explain the associated pterygoid plate shape that is wide and laterally flaring as it is the area of insertion of the medial pterygoid (Fig. 10 and Table 8) and the broad zygomatic arch and a wide temporal fossa that is the area of insertion of zygomatico-mandibularis (Fig. 10 and Table 8). The fact that strong co-variation was observed specifically with the PCSA data suggests that this is not due to spatial constraints (i.e. space needed to put or attach big muscle) but rather reflects a functional co-variation suggesting that bone is remodeled to be able to resist the muscle forces exerted upon them during chewing.

The main unexpected results of this study are the low correlation and co-variation between mandibular shape and the masticatory muscles. Indeed, the masticatory muscles impact mandibular shape only as represented by the third PC axis (accounting for 7% of the variance). Furthermore, only little co-variation between masticatory muscles and mandibular shape was observed. There

TABLE 8. General origin and insertion of the muscles (from Perry, 2008) depicted in Figure 10

	Origin	Insertion
Superficial Masseter	It originates from the ventral margin of the zygomatic arch and from the ventral half of lateral surface of zygomatic arch.	It inserts: - posteriorly onto the angular process of the mandible; - onto the lateral surface and on the ventral and posterior borders of the mandibular ramus; - sometimes, onto the posterior surface of the lateral pole of the mandibular condyle.
Deep Masseter	It originates from the ventral surface of the zygomatic arch, the zygomatic process of the temporal posteriorly and from the zygomatic process of the maxilla anteriorly.	It inserts onto the bones of the ascending ramus of the mandible and onto fibers of the deep masseter fascia.
Zygomatico-mandibularis	Inferior medial surfaces of the zygomatic arch, deep to the origin for the deep masseter.	Fibers of this muscle inserts into masseteric fossa, dorsal to insertion for the deep masseter. Its superficial anterior portion interdigitates with the deep masseter, while its deep portion interdigitated with the zygomatic temporalis. This muscle occupy the greatest surface area of attachment on the ascending ramus of the mandible.
Temporalis pars-suprazygomatica	Lateral to the superficial temporalis, from the medial and dorsal aspect of the zygomatic arch, where the arch comprises a concave trough	It inserts on the lateral aspect of coronoid process of the mandible.
Superficial Temporalis	It originates from the temporal fossa (frontal, parietal and squamosal bones). One fascia is attached dorsally as the superior temporal line and as far as the nuchal crest, it also attach the dorsal margin of the zygomatic arch	It inserts onto the antero-lateral aspect of the coronoid process of the mandible and onto a tendon that inserts on the anterior border of the coronoid process and a pit behind the last lower molar.
Deep Temporalis	It originates from the entire temporal fossa, as far ventrally as a prominent horizontal ridge that runs from the posterior root of the zygomatic arch to the medial wall of the orbit near the optic foramen	It inserts onto the medial aspect of the coronoid process, from the anterior border to the posterior border of the mandible. Fibers that are more dorsal and anterior insert on the temporal tendon. Fibers insert onto the surface of the braincase.
Medial Pterygoid	It originates from two locations: - the medial surface of the lateral pterygoid plate; - the oval depression in the sphenoid bone of the medial wall of the orbit	It inserts on the medial surface of the angular process of the mandible

is a tendency for co-variations to be significant on the third PLS axis for the PCSA and the co-variation is significant on the third and fourth PLS axis for volume (both axes accounting for a small percent of the co-variance). These results were not as predicted. Interestingly, it appears that there is the group of the frugivorous and insectivorous species that co-vary together and, a group of the leaf eaters (*Propithecus* and *Hapalemur*) and the really specialized aye-aye (*D. madagascariensis*) that also co-vary together. Indeed, this last group (leaf and hard objects eater species) seems to have two different ways to combine strong masticatory muscles in association with two different mandibular morphotypes: (1) the aye-aye (*D. madagascariensis*) morphotype representing a hard object eater, with an angular process that is less developed, with a wide and vertically oriented coronoid process, an articulation of the mandible with the cranium that is posteriorly oriented and a robust ramus associated with a strong deep temporalis, superficial masseter and temporalis; (2) the folivore morphotype (*Hapalemur* and *Propithecus*), with a wide angular process, an elongated coronoid process, an articulation of the mandible with the cranium that is vertically oriented and a more gracile ramus associated with a strong zygomatico-mandibularis and medial pterygoid. These two different associations between strong masticatory muscles and mandibular shape may "hide" or mask the co-variation between the mandibular shape and the masticatory muscles but represent the functional constraints of gnawing at large gape in the aye-aye versus the chewing of leaves at low gape. We presume that much of this pattern is driven by the unique morphology (and feeding behavior) of the aye-aye. This taxon is not only very derived in its mandibular morphology, it is also the sister taxon of all other lemuriforms with a very deep divergence. In order to assess the effect of the highly

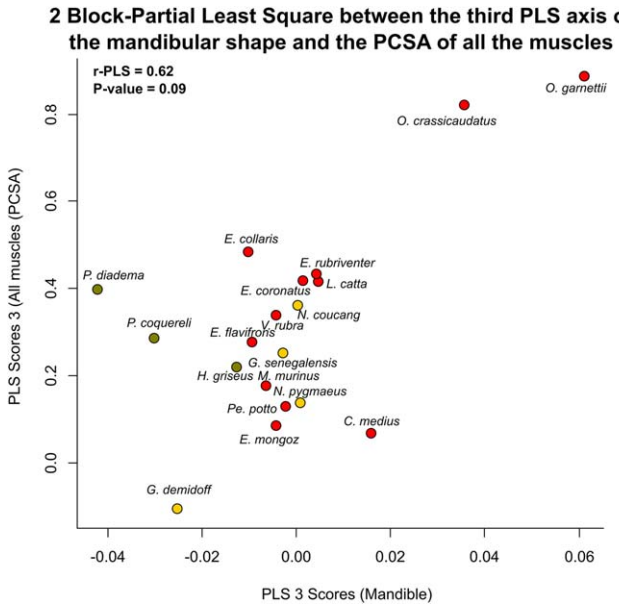

Fig. 11. Results of the 2B-PLS between the mandibular shape and the PCSA of the masticatory muscles without the aye-aye. Scatter plot of the third PLS axis describing the shape co-variation between mandibular shape and the PCSA of the masticatory muscles. Color code of the points in the scatterplot represents the diet of each species with: red points representing frugivores, green khaki points representing folivores, yellow points represent insectivores, and black point representing the aye-aye.

specialize aye-aye, we performed the same co-variation analyze excluding the aye-aye (Fig. 11). The co-variations are still not significant and remain rather similar, with a group of the frugivorous and insectivorous species that co-vary together and, a group of the leaf eaters (*Propithecus* and *Hapalemur*) that also co-vary, however, outside of the main co-variation occupied by the frugivorous and insectivorous species (Fig. 11).

More generally, because the mandible is presumably less constrained by non-dietary factors than is the cranium, we predicted that co-variation between the mandible and aspects of diet would be tighter than between the cranium and diet. The opposite was, however, observed. Futhermore, our results also show that the mandible is more disparate than the cranium in strepsirrhines. Perhaps it is the very lack of connection between the mandible and non-dietary systems that permits it to vary in strepsirrhines. Due to a lack of other constraints, mandibular morphology may more subject to random variation through, for example, genetic drift. By contrast, the cranium is tightly integrated by virtue of its role in housing the brain and sensory systems (Wake and Roth, 1989; Hanken and Hall, 1993) which may constraint the covariation patterns.

The pattern of co-variation seen between the muscles and the cranium is interesting because insectivorous strepsirrhines are clearly different from folivorous ones—a difference that is not always recovered by dental signals (e.g. Kay, 1975; Kay and Sheine, 1979; Chivers et al., 1984; Kay et al., 2004; Marshall and Wrangham, 2007; Ramdarshan et al., 2011). The division of the frugivores into two groups highlights the importance of secondary food sources. The one group is composed of small-bodied forms that acquire their protein primarily from insects (*Cheirogaleus*, *Perodicticus*, and *Microcebus*) and the other is composed of larger-bodied forms that acquire their protein primarily from leaves (*Eulemur* and *Varecia*) or opportunistic gummivory (*Otolemur*) (Chivers et al., 1984; Fleagle, 1999; White, 2009; Ramdarshan et al., 2011). Thus there is likely an important role of tough foods in determining chewing muscle dimensions and cranial form.

The pattern of individual muscle variation is also significant in identifying which muscles are important for processing leaves versus insects. The muscles that covary the most with variation along a folivore-insectivore axis are the deepest layers of the masseter (especially zygomatico-mandibularis) and the medial pterygoid. Notably, these muscles are likely very important in generating horizontal movements (and contributing to horizontal bite loads) and are expected to be larger and stronger in strepsirrhines that process tough, flat foods like leaves. This pattern supports preliminary observations by Perry et al. (2011) on the division of labor in the chewing musculature of strepsirrhines.

ACKNOWLEDGEMENTS

The authors would like to thank two anonymous reviewers for constructive comments on a previous version of the manuscript. We thank J Cuisin, C Bens and A Verguin for access to the specimens from the collections Anatomie Comparée, MNHN. E Gilissen and W Wendelen for access to the specimens from the collections of the Royal Museum of Central Africa, Tervuren, Belgium. We also thank MorphoSource for making scans available. Lynn Lucas and Lynn Copes provided access to these data, the acquisition of which was supported by NSF DDIG no. 0925793 and the Wenner Gren Foundation. We thank the Smithsonian's Division of Mammals (Dr. Kristofer Helgen) and Human Origins Program (Dr. Matt Tocheri) for the scans of USNM specimens used in this research (http://humanorigins.si.edu/evidence/3d-collection/primate). These scans were acquired through the generous support of the Smithsonian 2.0 Fund and the Smithsonian's Collections Care and Preservation Fund. We thank Amandine Blin and Michel Baylac from the "plate-forme de morphométrie" of the UMS 2700 (CNRS, MNHN) for access to the surface scanner. A.C.F. thanks the Marie-Skłodowska Curie fellowship (EU project 655694 – GETAGRIP) for funding. The authors also thank R Cornette and DC Adams for their helpful discussions on this manuscript.

AUTHOR CONTRIBUTIONS

A.C.F. conceived the paper, performed the data acquisition and analysis, and drafted the manuscript. MD helped to conceive the paper, with data acquisition and to draft the manuscript. J.M.G.P. and A.H.R. helped to conceive the paper and drafted the manuscript. A.L. and A.B. helped to perform the acquisition of data. The authors have no conflicts of interest to declare.

LITERATURE CITED

Adams DC. 2014. A generalized K statistic for estimating phylogenetic signal from shape and other high dimensional multivariate data. Syst Biol 63:685–697.

Adams DC, Felice RN, Kamilar JM. 2014. Assessing phylogenetic morphological integration and trait covariation in morphometric data using evolutionary covariance matrices. PLoS One 9:e94335.

Adams DC, Otárola-Castillo E, Paradis E. 2013. Geomorph: an R package for the collection and analysis of geometric morphometric shape data. Methods Ecol Evol 4:393–399.

Baab KL, Perry MG, Rohlf FJ, Jungers WL. 2014. Phylogenetic, ecological, and allometric correlates of cranial shape in Malagasy lemuriforms. Evolution 68:1450–1468.

Blomberg SP, Garland T, Jr, Ives AR. 2003. Testing for phylogenetic signal in comparative data: behavioural traits are more labile. Evolution 57:717–745.

Bock WJ, von Wahlert G. 1965. Adaptation and the form-function complex. Evolution 19:269–299.

Bookstein FL. 1997. Landmark methods for forms without landmarks: morphometrics of group differences in outline shape. Med Image Anal 1:225–243.

Bookstein FL, Gunz P, Mitteroecker P, Prossinger H, Schaefer K, Seidler H. 2003. Cranial integration in Homo: singular warps analysis of the midsagittal plane in ontogeny and evolution. J Hum Evol 44:167–187.

Chivers DJ, Wood BA, Bilsborough A. 1984. Food acquisition and processing in primates. New York: Plenum.

Cock AG. 1966. Genetical aspects of metrical growth and form in animals. Quart Rev Biol 41:131–190.

Cornette R, Baylac M, Souter T, Herrel A. 2013. Does shape covariation between the skull and the mandible have functional consequences? A 3D approach for a 3D problem. J Anat 223:329–336.

Cornette R, Tresset A, Herrel A. 2015. The shrew tamed by Wolff's law: do functional constraints shape the skull through muscle and bone covariation? J Morphol 276:301–309.

Currey JD. 2002 Bones: Structure and mechanics. Princeton: Princeton University Press.

Dumont M, Wall CE, Botton-Divet L, Goswami A, Peigné S, Fabre A-C. 2016. Do functional demands associated with locomotor habitat, diet, and activity pattern drive skull shape evolution in musteloid carnivorans?. Biol J Linn Soc 117:858–878.

Eng CM, Lieberman DE, Zink KD, Peters MA. 2013. Bite force and occlusal stress production in Hominin evolution. Am J Phys Anthropol 151:544–557.

Fabre A-C, Cornette R, Slater G, Argot C, Peigné S, Goswami A, Pouydebat E. 2013a. Getting a grip on the evolution of grasping in musteloid carnivorans: a three-dimensional analysis of forelimb shape. J Evol Biol 26:1521–1535.

Fabre A-C, Cornette R, Peigné S, Goswami A. 2013b. Influence of body mass on the shape of forelimb in musteloids carnivorans. Biol J Linn Soc 110:91–103.

Fabre A-C, Andrade DV, Huyghe K, Cornette R, Herrel A. 2014a. Interrelationships between bones, muscles, and performance: biting in the lizard *Tupinambis merianae*. Evol Biol 41:518–527.

Fabre A-C, Goswami A, Peigné S, Cornette R. 2014b. Morphological integration in the forelimb of musteloid carnivorans. J Anat 225: 19–30.

Fabre A-C, Cornette R, Goswami A, Peigné S. 2015a. Do constraints associated with the locomotor habitat drive the evolution of forelimb shape? A case study in musteloid carnivorans. J Anat 226: 596–610.

Fabre A-C, Salesa MJ, Cornette R, Antón M, Morales J, Peigné S. 2015b. Quantitative inferences on the locomotor behaviour of extinct species applied to *Simocyon batalleri* (Ailuridae, Late Miocene, Spain). Sci Nat 102:30.

Felsenstein J. 1985. Phylogenies and the comparative method. Am Nat 125:1–15.

Fleagle JF. 1999. Primate adaptation and evolution, 2nd ed. New York: Academic Press.

Grüneberg H. 1967. The pathology of development: a study of inherited skeletal disorders in animals. Oxford: Blackwell.

Gunz P, Mitteroecker P. 2013. Semilandmarks: a method for quantifying curves and surfaces. Hystrix 24:103–109.

Gunz P, Mitteroecker P, Bookstein FL. 2005. Semilandmarks in three dimensions. In: Slice DE editor. Modern morphometrics in physical anthropology. Berlin: Springer. p 73–98.

Hanken J, Hall BK. 1993. The skull, volume 3: functional and evolutionary mechanisms. Chicago: University of Chicago Press.

Harvey PH, Pagel MD. 1991. The comparative method in evolutionary biology. Oxford: University Press Oxford.

Herrera JP, Dávalos LM. 2016. Phylogeny and divergence times of lemurs inferred with recent and ancient fossils in the tree. Syst Biol 65:772–791.

Hornik K. 2015. *The R FAQ*. https://CRAN.R-project.org/doc/FAQ/R-FAQ.html

Kay RF. 1975. The functional adaptations of primate molar teeth. Am J Phys Anthropol 43:195–215.

Kay RF, Sheine WS. 1979. On the relationship between chitin particle size and digestibility in the primate *Galago senegalensis*. Am J Phys Anthropol 50:301–308.

Kay RF, Schmitt DO, Vinyard CJ, Perry JMG, Shigehara N, Takai M, Egi N. 2004. The paleobiology of Amphipithecidae, South Asian late Eocene primates. J Hum Evol 46:3–25.

Lieberman DE, Krovitz GE, Yates FW, Devlin M, St. Claire M. 2004. Effects of food processing on masticatory strain and craniofacial growth in a retrognathic face. J Hum Evol 46:655–677.

Marshall A, Wrangham R. 2007. Evolutionary consequences of fallback foods. Int J Primatol 28:1219–1235.

Meloro C, Cáceres NC, Carotenuto F, Sponchiado J, Melo GL, Passaro F, Raia P. 2015. Chewing on the trees: Constraints and adaptation in the evolution of the primate mandible. Evolution 69:1690–1700.

Noback ML, Harvati K. 2015. Covariation in the human masticatory apparatus. Anat Rec 298:64–84.

Oxnard CE. 2008. Ghostly muscles, wrinkled brains, heresies and hobbit. A Leverhulme Public Lectures Series. Singapore: World Scientific.

Parr WCH, Wroe S, Chamoli U, Richards HS, McCurry MR, Clausen PD, McHenry C. 2012. Toward integration of geometric morphometrics and computational biomechanics: New methods for 3D virtual reconstruction and quantitative analysis of Finite Element Models. J Theor Biol 301:1–14.

Perry JMG. 2008. The anatomy of mastication in extant strepsirrhines and Eocene adapines. Ph.D., Duke University.

Perry JMG, Hartstone-Rose A, Wall C. 2011. The Jaw adductors of Strepsirrhines in relation to body size, diet, and ingested food size. Anat Rec 294:712–728.

Perry JMG, Macneill KE, Heckler AL, Rakotoarisoa G, Hartstone-Rose A. 2014. Anatomy and adaptations of the chewing muscles in *Daubentonia* (Lemuriformes). Anat Rec 297:308–316.

Perry JMG, St Clair EM, Hartstone-Rose A. 2015. Craniomandibular signals of diet in Adapids. Am J Phys Anthropol 158:646–662.

Polly PD. 2008. Adaptive zones and the pinniped ankle: A 3D quantitative analysis of carnivoran tarsal evolution; pp. 165–194 in E Sargis and M Dagosto (eds.) Mammalian evolutionary morphology: a tribute to Frederick S. Szalay. Dordrecht: Springer.

Ramdarshan A, Merceron G, Marivaux L. 2012. Spatial and temporal ecological diversity amongst Eocene primates of France: evidence from teeth. Am J Phys Anthropol 147:201–216.

Renaud S, Auffray JC, De La Porte S. 2010. Epigenetic effects on the mouse mandible: common features and discrepancies in remodelling due to muscular dystrophy and response to food consistency. BMC Evol Biol 10:28.

Rohlf FJ, Corti M. 2000. Use of two-block partial least-squares to study covariation in shape. Syst Biol 49:740–753.

Rohlf FJ, Slice D. 1990. Extensions of the Procrustes method for the optimal superimposition of landmarks. Syst Biol 39:40–59.

Schlager S. 2013. Morpho: Calculations and visualizations related to Geometric Morphometrics. R Package Version 21–1141011.

Singh N, Harvati K, Hublin J-J, Klingenberg CP. 2012. Morphological evolution trough integration: a quantitative study of cranial integration in *Homo*, *Pan*, *Gorilla* and *Pongo*. J Hum Evol 62:155–164.

Stedman HH, Kozyak BW, Nelson A, Thesier DM, Su LT, Low DW, Bridges CR, Shrager JB, Minugh-Purvis N, Mitchell MA. 2004. Myosin gene mutation correlates with anatomical changes in the human lineage. Nature 428:415–418.

Terhune CE, Cooke SB, Otárola-Castillo E. 2015. Form and function in the platyrrhine skull: a three-dimensional analysis of dental and TMJ morphology. Anat Rec 298:29–47.

Thorpe RS. 1981. The morphometrics of the mouse: a review. In: Berry RJ editor. Biology of the house mouse. London: Zool Soc London. p 85–125.

Toro-Ibacache V, Muñoz VZ, O'Higgins P. 2016. The relationship between skull morphology, masticatory muscle force and cranial skeletal deformation during biting. Ann Anat 203:59–68.

Viguier B. 2002. Is the morphological disparity of lemur skulls (Primates) controlled by phylogeny and/or environmental constraints? Biol J Linn Soc 76:577–590.

Viguier B. 2004. Functional adaptations in the craniofacial morphology of Malagasy primates: shape variations associated with gummivory in the family Cheirogaleidae. Ann Anat 186:495–501.

Wake DB, Roth G. 1989. Complex organismal functions: integration and evolution in vertebrates. New York: Wiley & Sons Wiley.

White J. 2009. Geometric morphometric investigation of molar shape diversity in modern lemurs and lorises. Anat Rec 292:701–719.

Wiley DF, Amenta N, Alcantara DA, Ghosh D, Kil YJ, Delson E, Harcourt-Smith W, Rohlf FJ, St John K, Hamann B. 2005. Evolutionary morphing. In: *Proceedings of IEEE Visualization 2005 (VIS'05)*, 23–28 October 2005. Minneapolis, MN, USA.

Wroe S, Ferrara TL, McHenry CR, Curnoe D, Chamoli U. 2010. The craniomandibular mechanics of being human. Proc R Soc London Ser B 277:3579–3586.

Zelditch LM, Swiderski DL, Sheets HD. 2012. Geometric morphometrics for biologists, a primer, 2nd ed. San Diego, USA: Academic Press.